REPORT DOCUMENTATION PAGE

Form Approved
OMB No. 0704-0188

1. AGENCY USE ONLY (Leave blank)	2. REPORT DATE	3. REPORT TYPE AND DATES COVERED
		FINAL REPORT - 30 Sep 93 - 31 Dec 96

4. TITLE AND SUBTITLE
(DEPSCOR-92) Ultrafast Pulsed Applications to Photonic Device Materials and MBE Growth Research

5. FUNDING NUMBERS
61103D
3484/BS

6. AUTHOR(S)
Professor Jin-Joo Song

AFOSR-TR-97-

7. PERFORMING ORGANIZATION NAME(S) AND ADDRESS(ES)
Center for Laser and Photonics Research
Department of Physics
Oklahoma State University
413 Noble Research Center
Stillwater, OK 74078

8. PERFORMING ORGANIZATION REPORT NUMBER
0157

9. SPONSORING/MONITORING AGENCY NAME(S) AND ADDRESS(ES)
AFOSR/NE
110 Duncan AVenue Suite B115
Bolling AFB DC 20332-8050

10. SPONSORING/MONITORING AGENCY REPORT NUMBER
F49620-93-1-0510

11. SUPPLEMENTARY NOTES

12a. DISTRIBUTION/AVAILABILITY STATEMENT
APPROVED FOR PUBLIC RELEASE: DISTRIBUTION UNLIMITED

12b. DISTRIBUTION CODE

13. ABSTRACT *(Maximum 200 words)*

The research performed centered around the establishment of state-of-the-art time-domain spectroscopy capabilities. This included the upgrade of a femtosecond Ti:sapphire with second-harmonic generation to less than 350 nm for studying wide-bandgap III-N semiconductors in the ultraviolet spectral range. Probing of the optical properties of III-N structures proceeded, resulting in a significant initial data base for this new material system. In addition, femtosecond four-wave-mixing signals were observed for the first time in GaN, leading to an understanding of phonon-exciton interactions leading to exciton line broadening. This work led to collaborations with a large group of researchers in the III-N community, and became the basis for expanded funding.

14. SUBJECT TERMS

15. NUMBER OF PAGES

16. PRICE CODE

17. SECURITY CLASSIFICATION OF REPORT	18. SECURITY CLASSIFICATION OF THIS PAGE	19. SECURITY CLASSIFICATION OF ABSTRACT	20. LIMITATION OF ABSTRACT
UNCLASSIFIED	UNCLASSIFIED	UNCLASSIFIED	

FINAL REPORT

Project Title: ULTRAFAST PULSED LASER APPLICATIONS TO PHOTONIC DEVICE MATERIALS AND MBE GROWTH

Principal Investigator: Dr. Jin-Joo Song
Center for Laser and Photonics Research &
Department of Physics
413 Noble Research Center
Oklahoma State University
Stillwater, OK 74078
405-744-6575

Grant No: F49620-93-1-0510

Contracting Period: 30 September 1993 - 31 December 1996

FINAL EQUIPMENT REPORT

This AFOSR award, "Ultrafast Pulsed Laser Applications to Photonic Device Materials and MBE Growth," included cost share funds from the University in the amount $110,920.

A state-of-the-art Hamamatsu streak camera was procured for time-domain spectroscopy. Also, our femtosecond Ti:Sapphire laser was upgraded to generate second harmonic beams in the UV range for our wide-gap semiconductor research, especially III-nitrides. In order to save on costs, we assembled our apparatus instead of purchasing a commercial unit. The optical and mechanical parts had to be purchased. Especially, there is no efficient commercial unit for generation of the femtosecond second harmonic beam in the range of our interest, <350 nm.

This equipment has been used successfully in probing the optical properties of GaN and related structures such as InGaN and AlGaN/GaN DH structures. The projects yielded many important results as shown in the attached reprints and preprints. The students involved in the research received truly unique training in the laser technology, as well as in the III-nitride carrier dynamics in the picosecond range.

We have also successfully observed femtosecond four-wave-mixing signals for the first time in GaN. This work is very important in understanding exciton line broadening mechanisms, exciton-acoustic phonon, exciton-LO phonon interactions. This work also opens a new area of research in nitride quantum well excitons and their potential opto-electronic device applications.

Particularly significant in this work is that we collaborated with a large group of university and industry laboratories. They include Honeywell, CREE, EMCORE, North Carolina State University (Prof. S. Bedair and Prof. R. Davis) and University of Illinois (Prof. H. Morkoc and Prof. Y.C. Chang).

We plan to extend our collaboration network further to include Japanese research groups.

Also noteworthy is that the apparatus procured with this award was the basis for attracting other external funding including the following:

DEPSCOR "Ultrafast Laser Investigations of GaN Based Semiconductors for Device Applications" 9/1/96 to 8/31/99 $339,000

DURIP "Instrumentation for Wide-gap III-Nitride Research: MOCVD Reactor & UV-Blue Femtosecond Laser Amplifier" 3/1/97 to 2/28/99 $300,000

DARPA/ AASERT "Nonlinear Optical Investigations of Wide Bandgap Semiconductors for Optoelectronic Device Applications" 6/1/96 to 5/31/99 $137,227.

With the establishment of an up-to-date MOCVD facility within this year, the equipment procured will further accelerate GaN-related research, both fundamental and applied, especially in UV-blue photonic materials and device development.

The following are publications related to the project "Ultrafast Pulsed Laser Applications to Photonic Device Materials and MBE Growth."

"Time-resolved Exciton Luminescence in GaN Grown by Metalorganic Chemical Vapor Deposition", W.Shan, X.C. Xie, J.J. Song, and B. Goldenberg, Appl. Phys. Lett. **67**, 2512 (1995).

"Optical Properties of Wurzite GaN Grown by Low-pressure Metalorganic Chemical-Vapor Deposition", W. Shan, T. Schmidt, X.H. Yang, J.J. Song, and B. Goldenberg, J. Appl. Phys. **79**, 3691 (1996).

"Optical Studies of Epitaxial GaN Based Materials", J.J. Song, W. Shan, T. Schmidt, X.H. Yang, A. Fischer, S.J. Hwang, B. Taheri, B. Goldenberg, R. Horning, A. Salvador, W. Kim, O. Aktas, A. Botchkarev, and H. Morkoc, SPIE Proceedings, **2693**, 86 (1996).

"Optical Studies of GaN and GaN/AlGaN Heterostructures on SiC Substrates", W. Shan, A.J. Fischer, J.J. Song, G.E. Bulman, H.S. Kong, M.T. Leonard, W.G. Perry, M.D. Bremser, and R.F. Davis, Appl. Phys. Lett. **69**, 740 (1996).

"Optical Transitions in $In_xGa_{1-x}N$ Alloys Grown by Metalorganic Chemical Vapor Deposition", W. Shan, B. Little, J.J. Song, Z.C. Feng, M. Schurman, and R.A. Stall, Appl. Phys. Lett. **69**, 3315 (1996).

"Recent Progress in Optical Studies of Wurzite GaN Grown by Metalorganic Chemical Vapor Deposition", W. Shan, T. Schmidt, X.H. Yang, J.J. Song, and B. Goldenberg, Inst. Phys. Conf. Ser. **145**, 1151 (1996).

"Femtosecond Four-Wave-Mixing Studies of Nearly Homogeneously Broadened Excitons in GaN", A.J. Fischer, W. Shan, G.H. Park, J.J. Song, D.S. Kim, D.S. Yee, R. Horning, and B. Goldenberg, submitted to Phys. Rev. B, 1997.

Time-resolved exciton luminescence in GaN grown by metalorganic chemical vapor deposition

W. Shan,[a] X. C. Xie, and J. J. Song
Department of Physics and Center for Laser Research, Oklahoma State University, Stillwater, Oklahoma 74078

B. Goldenberg
Honeywell Technology Center, Plymouth, Minnesota 55441

(Received 26 June 1995; accepted for publication 15 August 1995)

We report the results of time-resolved studies on the exciton radiative decay in single-crystal GaN films grown by metalorganic chemical vapor deposition. Time-resolved photoluminescence (PL) measurements were performed on the samples at various temperatures from 10 to 320 K. The well-resolved near-band-edge luminescence features associated with free excitons and bound excitons in the GaN allow us to unambiguously determine their decay times. We found that the nonradiative recombination processes play an important role and dominate the decay of exciton population. The processes depend on the density of defects and impurities in the GaN samples. © *1995 American Institute of Physics.*

GaN-based III–V nitride semiconductors currently attract extensive attention for their potential device applications.[1–3] Superbright high-efficient blue LEDs based on nitride structures have been demonstrated by the Nichia group and others.[4] The observation of optically pumped laser action in GaN with clear resolvable longitudinal lasing modes over a broad temperature range from 10 to 400 K has been recently reported by a few research groups.[5,6] All this progress has led to much more intense interest in the development of efficient nitride UV-visible light emitters. In this letter, we represent the results of time-resolved studies of nonresonantly excited exciton luminescence in single-crystal GaN epilayer films grown on sapphire substrates by metalorganic chemical vapor deposition. The intrinsic free-exciton (FX) luminescence line in the samples used in this work can be spectrally well resolved from that of excitons bound to neutral donors (BX). This allows us to unambiguously study the recombination dynamics of both intrinsic free excitons and neutral-donor bound excitons.

The GaN samples used in this work were nominally undoped single-crystal films grown by metalorganic chemical vapor deposition on (0001) sapphire substrates.[3] The thickness of the GaN epilayers used in this work ranges from 2.5 to 7 μm. Time-integrated photoluminescence (TIPL) measurements were first performed to characterize the GaN samples. The experimental setup for the TIPL measurements consisted of a HeCd laser as an excitation source and a 1.0-M double-grating monochromator with a photon counting and data acquisition system. For time-resolved photoluminescence (TRPL) measurements, the primary excitation source was a pulsed dye laser synchronously pumped by a frequency-doubled mode-locked Nd:YAG laser (82 MHz). The output laser pulses from the dye laser with a pulse duration of less than 5 ps and at the wavelength around 600 nm was then frequency doubled into UV pulses by a nonlinear crystal. The luminescence signals were dispersed by a 1/4 M monochromator and detected by a synchronscan streak camera with a temporal resolution of 2 ps. The detection system provides the capabilities of simultaneously measuring photoluminescence intensity, time, and wavelength. The overall time resolution of the system is less than 15 ps.

Time-integrated photoluminescence spectra taken from the samples used in this work all exhibit strong, predominant near-band-edge exciton luminescence lines and a weak broadband emission structure peaked at yellow spectral regions. Another weak broadband emission centered at the blue color range could be also detected. The inset of Fig. 1 shows a typical time-integrated PL spectrum taken at 10 K. Two

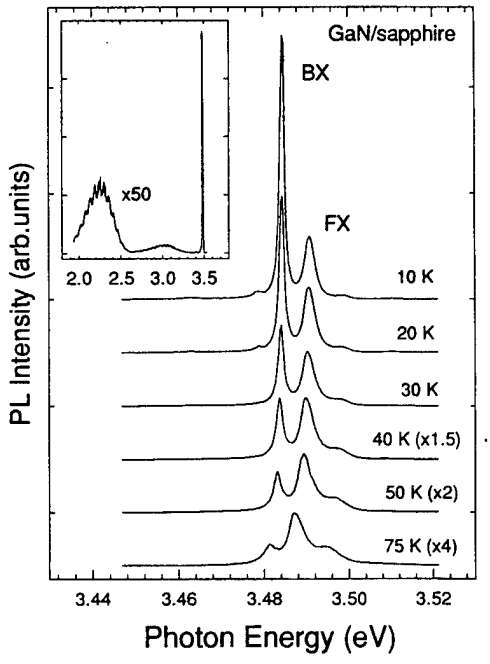

FIG. 1. Time-integrated exciton luminescence spectra of a MOCVD GaN sample taken at different temperatures. The inset shows the 10 K PL spectrum of the sample over a broad spectral range.

[a]Electronic mail:wshan@osuunx.ucc.okstate.edu

 0003-6951/95/67(17)/2512/3/$6.00

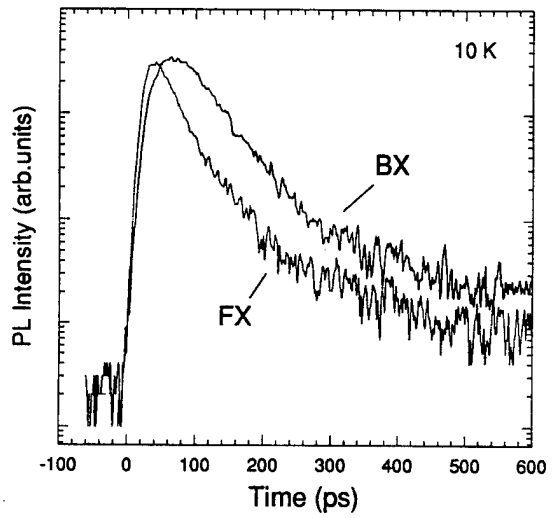

FIG. 2. Temporal variation of spectrally integrated PL for both intrinsic free-exciton and bound-exciton emissions.

sharp luminescence lines dominate near-band-edge emission spectra. The strongest emission line marked by BX in Fig. 1 has a full width at half maximum (FWHM) of less than 1.0 meV at 10 K. The second one labeled FX in the figure shows a FWHM of less than 1.5 meV. The intensity of the BX peak was found to decrease with increasing temperature much faster than that of FX as shown in Fig. 1, where the near-band-edge PL spectral features were plotted as a function of temperature. It became hardly resolvable when the temperature was raised to above 100 K (not shown). Such effects of temperature on the luminescence intensity indicate the emission line resulting from radiative recombination of excitons bound to neutral donors.[7] The rapid thermal quenching below 100 K implies that the exciton is bound very weakly; hence it must be bound to a shallow neutral donor, not a deep donor, or an acceptor. The second strongest luminescence line (FX), together with the weak emission feature on the higher energy side, can be attributed to intrinsic free-exciton emissions associated with the split-off band states of GaN due to the symmetry of the wurtzite structure.[8]

Figure 2 illustrates the temporal evolution of spectrally integrated exciton luminescence for both free-exciton and bound-exciton emissions observed in a GaN sample at 10 K. The time evolution for both free-exciton and bound-exciton luminescence is dominated by exponential decay. A much weaker long-decay component with an intensity more than two decades smaller compared to the main process could also be observed at low temperatures. The lifetime of the main PL decay was found to be ~35 ps for the free-exciton emissions and ~55 ps for the bound-exciton emissions for the GaN sample at 10 K. It has to be pointed out that the measurement of luminescence decay time does not provide a direct measurement of radiative lifetime, the measured PL decay time only yields an effective lifetime (τ_{eff}) for free excitons and bound excitons. It involves both the radiative (τ_R) and nonradiative (τ_{NR}) lifetimes with the decay rate expressed as

$$1/\tau_{\text{eff}} = 1/\tau_R + 1/\tau_{\text{NR}}. \tag{1}$$

In this equation we have assumed that the nonradiative decay mechanism is linear, so that a lifetime can be defined. The radiative lifetime for an excited state in a semiconductor can be estimated by considerations of optical transition probability. The radiative lifetime τ_R of the excited state can be described by[9,10]

$$\tau_R = 2\pi\epsilon_0 m_0 c^3/\tilde{n}e^2\omega^2 f, \tag{2}$$

where f is the oscillator strength of the optical transition, $\tilde{n}$ is the refractive index, and the other symbols have their usual meanings. By using $\tilde{n}=2.4$,[11] and $\omega=\sim 5.3\times 10^{15}$ s^{-1} for GaN, one can roughly obtain $\tau_R \sim (800/f)$ ps. The radiative lifetime of bound excitons in GaN is thus expected to be just a little shorter than 1 ns and on the order of several hundreds of picoseconds if we take the upper limit with its oscillator strength as unity ($f\sim 1$). The oscillator strength of free excitons calculated within the effective-mass approximation is given by $f = E_p/\pi\hbar\omega(V/a_x^3)$, where E_p is the Kane matrix element connecting Bloch states in the valence and conduction bands, V is the volume of unit cell, and a_x is the effective Bohr radius of free exciton. Our result yields $f\sim 0.012$ for the free excitons in GaN using $E_p \sim 18$ eV and $a_x \sim 20$ Å.[12] Thus, the calculated value of the radiative lifetime for free excitons in GaN will be in the several tens of nanoseconds domain.

Generally, the discrepancy between the measured values of PL decay time and the theoretical estimated radiative lifetime can be attributed to nonradiative relaxation processes in competition with the radiative channel. For the case where the nonradiative decay rate is larger, the measured decay time is characteristic for the nonradiative processes in accordance with Eq. (1). This situation is typical for recombination from intrinsic states of semiconductors.[13] The nonradiative processes such as multiphonon emission, capture by deep centers, Auger effect, etc. give rise to fast relaxation of the excited carriers down to lower states from which they decay radiatively or relax nonradiatively. As a result, the measured PL decay time for a given excited state is an effective lifetime and usually much shorter than a radiative one. This has been observed in a number of semiconductor bulk materials and heterostructures with the measured free-exciton PL decay time decreasing progressively as the density of nonradiative recombination centers increased.[14–16] The slow rise of bound-exciton luminescence intensity compared to that of the free-exciton PL shown in Fig. 2 is an indicator of such nonradiative relaxation processes for free excitons arriving at the bound-exciton energy. Therefore the capture of excitons and trapping of carriers by such nonradiative centers at defects and impurities must play a major role in the recombination processes responsible for the exciton population decay in the GaN samples studied in this work. In fact, the measured PL decay time was found to be directly related to the intensity of broadband emissions lying in the GaN band gap. The broad emission structure referred to as yellow emission in the literature is believed to be associated with the optical transitions between the energy levels involving impurity and/or defect states. The intensity of yellow emission is proportional to the density of some particular defects or impurities present in samples. We found that the

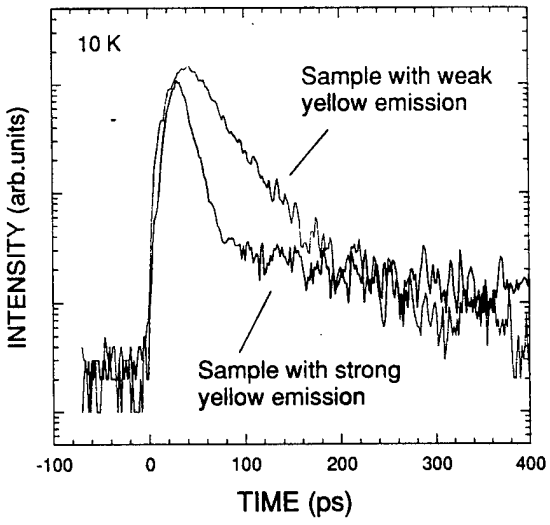

FIG. 3. Comparison of the time decay of free-exciton emission between two GaN samples with the relative intensity ratio of 100:1 for the yellow emission under the same excitation conditions.

stronger the yellow emission, the shorter the PL decay time in a GaN sample. Shown in Fig. 3 is a comparison of free-exciton PL decay between two samples with the relative intensity ratio of 100:1 for the yellow emission under identical excitation conditions. The deduced lifetime of free-exciton emission in the sample with stronger yellow emission is only 15 ps (which is the limit of our instrumental resolution). Therefore, the fast decay behavior of the PL intensity indicates that the capture of excitons and trapping of carriers at defects and impurities through nonradiative combinations dominate the decay of exciton population. The process of capture therefore must depend on the density of defects and impurities in the GaN samples.

The effects of sample temperature on the time decay of exciton luminescence were also examined. The bound-exciton PL decay time was found to decrease slightly with increasing temperature before the emission thermally quenched. The free-exciton PL decay time exhibited slow variations with temperature, either decreasing or increasing, from different samples. It is known that for a radiative recombination dominant system, an increase in the radiative lifetime with temperature is expected for the free excitons[10,17] since their average kinetic energy is increased. The thermal redistribution results in a decreasing number of the excitons close enough to the Brillouin-zone center for radiative recombination. Also the lifetime is expected to be independent of temperature for bound excitons, and only the emission intensity is expected to decrease because of thermal ionization of the bound excitons. Although recombination from excitons bound to extrinsic states such as defects or impurities can often be very efficient at low temperatures as demonstrated by Fig. 1, the measured decay time is still determined by detailed decay kinetics. The observed decreasing of PL decay time with temperature for the bound excitons in the GaN samples suggests that the incremental stronger nonradiative relaxations occur as the temperature is raised resulting in further faster decay of the exciton population. This can be also evidenced from the decrease of free-exciton PL intensity with temperature. Therefore, the variations of the measured PL decay time for free excitons with temperature in the GaN samples is a result of competition between nonradiative capture of free excitons at defects or impurities and thermally enhanced exciton–exciton and exciton–phonon scatterings.

In summary, we have performed time-resolved luminescence spectroscopy to study the exciton radiative decay in GaN epifilms grown by MOCVD. The decay time for both free-exciton and bound-exciton emissions was found to be quite short compared to the theoretical estimated radiative lifetime. The results suggest that the lifetime of excitons in the GaN samples is governed by nonradiative recombination. The capture of excitons and trapping of carriers at defects and/or impurities through nonradiative relaxation processes dominate the decay of exciton population. The capture process depends on the density of impurities and defects in the GaN samples.

This work was supported by AFOSR, ARPA, and ONR.

[1] S. Strite and H. Morkoç, J. Vac. Sci. Technol. B **10**, 1237 (1992), and references therein.
[2] J. I. Pankove, Mater. Res. Soc. Symp. Proc. **162**, 515 (1990), and references therein.
[3] H. Markoç, S. Strite, G. B. Gao, M. E. Lin, B. Sverdlov, and M. Burns, J. Appl. Phys. **76**, 1363 (1994), and references therein.
[4] See, for example, S. Nakamura, T. Mukai, and M. Senoh, Appl. Phys. Lett. **64**, 1687 (1994).
[5] X. H. Yang, T. J. Schmidt, W. Shan, J. J. Song, and B. Goldenberg, Appl. Phys. Lett. **66**, 1 (1995).
[6] A. S. Zubrilov, V. I. Mikolaev, V. A. Dmitriev, I. G. Irvine, J. A. Edmond, and C. H. Carter, Jr., Inst. Phys. Conf. Ser. No. 141, 525 (1995).
[7] R. Dingle, D. D. Sell, S. E. Stokowski, and M. Ilegems, Phys. Rev. B **4**, 1211 (1971).
[8] W. Shan, T. J. Schmidt, X. H. Yang, S. J. Hwang, J. J. Song, and B. Goldenberg, Appl. Phys. Lett. **66**, 985 (1995).
[9] D. L. Dexter, in *Solid State Physics*, edited by F. Seitz and D. Turnbull (Academic, New York, 1958), Vol. 6.
[10] G. W. 't Hooft, W. A. J. A. van der Poel, and L. W. Molenkamp, Phys. Rev. B **35**, 8281 (1987).
[11] *Landolt-Börnstein, New Series, Group III*, edited by O. Madelung (Springer, Berlin, 1982), Vol. 17.
[12] The effective Bohr radius of the free exciton in GaN was estimated by $a_x = 0.528(m_0\epsilon/\mu\epsilon_0)$ Å, where $\epsilon = \tilde{n}^2(\sim 5.8\epsilon_0)$, and μ is the reduced effective mass, $\sim 0.16 m_0$.
[13] M. Voos, R. F. Leheny, and J. Shah, in *Optical Properties of Solids*, edited by M. Balkanski (North-Holland, Amsterdam, 1980), Chap. 6, p. 336.
[14] C. J. Hwang, Phys. Rev. B **8**, 646 (1973).
[15] J. P. Bergman, P. O. Holtz, B. Monemar, M. Sundaram, J. L. Merz, and A. C. Gossard, Phys. Rev. B **43**, 4765 (1991).
[16] J. S. Massa, G. S. Buller, A. C. Walker, J. Simpson, K. A. Prior, and B. C. Cavenett, Appl. Phys. Lett. **64**, 589 (1994).
[17] J. Feldman, G. Peter, E. O. Göbel, P. Dawson, K. Moore, C. Foxon, and R. J. Elliott, Phys. Rev. Lett. **59**, 2337 (1987).

Optical properties of wurtzite GaN grown by low-pressure metalorganic chemical-vapor deposition

W. Shan,[a] T. Schmidt, X. H. Yang, and J. J. Song
Center for Laser Research and Department of Physics, Oklahoma State University, Stillwater, Oklahoma 74078

B. Goldenberg
Honeywell Technology Center, Plymouth, Minnesota 55420

(Received 20 October 1995; accepted for publication 18 December 1995)

We present the results of optical studies on the properties of GaN grown by low-pressure metalorganic chemical-vapor deposition, with emphasis on the issues vital to device applications such as stimulated emission and laser action as well as carrier relaxation dynamics. By optical pumping, stimulated emission and lasing were investigated over a wide temperature range up to 420 K. Using a picosecond streak camera, the free and bound exciton emission decay times were examined. In addition, the effects of temperature and pressure on the optical interband transitions and the transitions associated with impurity/defect states were studied using a variety of spectroscopic methods, including photoluminescence and photoreflectance. The fundamental band gap of GaN was mapped out as a function of temperature using the empirical Varshni relation. The pressure coefficient of the gap was determined using diamond-anvil pressure-cell technique. The hydrostatic deformation potential for the direct Γ band gap was also derived from the experimental results. © *1996 American Institute of Physics.* [S0021-8979(96)01907-6]

I. INTRODUCTION

GaN-based wide-band-gap III–V nitride semiconductors currently attract extensive attention for their potential electronic and optoelectronic device applications such as UV-blue light-emitting diodes (LEDs) and laser diodes.[1–3] With rapid progress in nitride epitaxial growth technology, high-quality nitride single-crystal epifilms can now be grown on such substrates as sapphire and SiC. Recent demonstration of superbright high-efficient blue LEDs based on nitride heterostructures by the Nichia group[4] and the reports on observation of optically pumped stimulated emission in GaN epifilms by a few groups[5,6] have led to much more intense interest in the development of efficient nitride UV-visible light emitters.

Although assessment of the properties and potential applications of nitrides is actively pursued to accelerate the device fabrication, some vital issues directly related to optoelectronic device applications such as optically pumped stimulated emission and lasing, as well as carrier dynamics, have not been widely addressed, and detailed studies on some important parameters associated with the electronic structures have not been fully explored. In this article we present the recent results of our spectroscopic studies on the optical properties of GaN grown by low-pressure metalorganic chemical-vapor deposition (MOCVD). A variety of experimental techniques was employed. The effects of temperature and pressure on the various optical transitions associated with both intrinsic and extrinsic processes in the GaN samples were examined by photoluminescence (PL) and photoreflectance (PR) spectroscopy. The variation of the fundamental band gap of GaN was mapped out as a function of temperature, and the energy value for the band gap of GaN at room temperature was obtained. The pressure coefficient of the GaN band gap was determined by studying the shift of exciton emission lines in GaN with applied pressure using the diamond-anvil pressure-cell technique. The deformation potential for the direct Γ band of GaN was also deduced from the experimental results. The dynamics of photoexcited excess carriers in high-quality GaN samples were investigated by transient luminescence spectroscopy in the picosecond regime using a streak camera in the region of near-band-edge excitonic emissions. We found that the strong capture of photoexcited carriers in impurities and/or defects through nonradiative recombination processes dominates the decay of carrier population. The capture process depends on the density of impurities and defects in the GaN samples. Optically pumped stimulated emission and lasing phenomena in GaN on sapphire were investigated using high-power pulsed lasers. Stimulated near-violet emissions were achieved with clearly observable longitudinal cavity modes over a wide temperature range from 10 up to 400 K.

II. EXPERIMENTAL DETAILS

The GaN samples used in this study were all nominally undoped epitaxial films grown on (0001) sapphire substrates by low-pressure MOCVD. Thin AlN buffers of ~50 nm were deposited on sapphire substrates at 775 °C before the growth of GaN. GaN layers with the thickness of a few microns (μm) were deposited at 1040 °C directly on the AlN buffers. These conditions typically result in high-quality single-crystal GaN layers. Various optical measurements were carried out on the GaN samples over a temperature range typically from 10 K to room temperature (295 K). Samples were mounted onto the cold finger of a closed-cycle refrigerator and cooled to desired temperatures for designated measurements. Conventional photoluminescence spec-

[a]Electronic mail: wshan@osuunx.ucc.okstate.edu

 0021-8979/96/79(7)/3691/6/$10.00

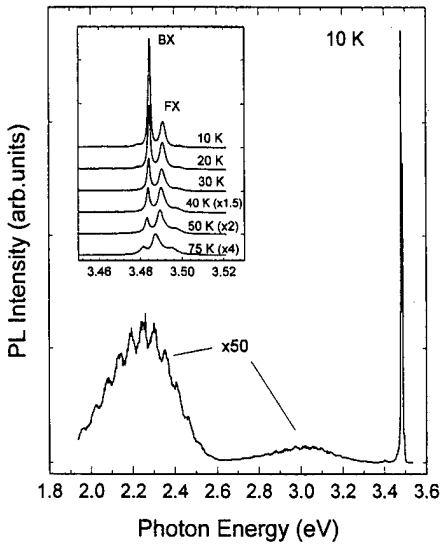

FIG. 1. Photoluminescence spectrum of a MOCVD GaN sample taken at 10 K. The inset shows the exciton luminescence spectra of the sample taken at different temperatures.

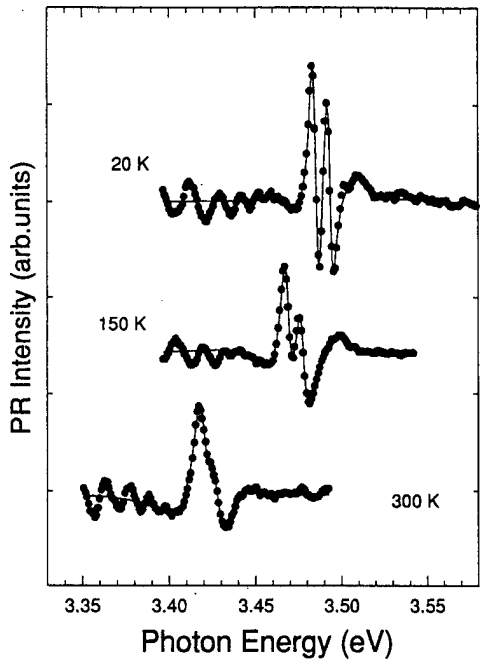

FIG. 2. Photoreflectance spectra of the GaN film at selected temperatures.

tra were measured using an experimental setup consisting of a cw HeCd laser (325 nm) as an excitation source and a 1 m double-grating monochromator connected with a photon-counting system. Time-resolved photoluminescence (TRPL) measurement was performed using a frequency-tunable pulsed laser with 2 ps pulse duration (82 MHz) as an excitation source and a streak camera with 2 ps time resolution in conjunction with a $\frac{1}{4}$ m monochromator as a detection system. Pressure-dependent PL measurement was conducted by using the diamond-anvil pressure-cell technique. For reflectance measurements, quasimonochromatic light dispersed by a $\frac{1}{2}$ m monochromator from a halogen-tungsten lamp was focused on the sample and the reflection signals were detected by a lock-in amplification system. Optical modulation was provided by chopping the HeCd laser beam when the PR measurements were performed. Stimulated emission and lasing experiment were carried out by employing side-pumping geometry. A frequency-doubled pulsed Nd:yttria aluminum garnet (YAG) laser (532 nm) with a repetition rate of 10 Hz was used to pump a dye laser as a primary optical pumping source (10 ns). The output of the dye laser was then frequency doubled into UV wavelengths to pump the GaN samples.

III. RESULTS AND DISCUSSIONS

To illustrate the quality and purity of the GaN epifilm samples used in this work, PL spectra taken from the samples are shown in Fig. 1. All GaN samples exhibit strong, predominant near-band-edge exciton luminescence lines corresponding to the radiative decay of excitons at low temperatures. Figure 1 shows a whole view of the typical PL spectrum taken at 10 K. The broadband yellow emission and a weak emission band in the blue spectral region could be observed. The strongest emission line marked by BX in Fig. 1 has a full width at half-maximum (FWHM) of less than 1.0 meV at 10 K. The second one labeled FX in the figure shows a FWHM of less than 1.5 meV, indicating the high quality as well as substantial purity of the samples. The intensity of the BX peak was found to decrease with increasing temperature much faster than that of FX. It became hardly resolvable when the temperature was raised to above 100 K (not shown). Such variations of the luminescence intensity as a function of temperature indicate the emission line can be attributed to the radiative recombination of excitons bound to neutral donors. The second strongest luminescence line, together with the weak emission feature on the higher-energy side, can be assigned to intrinsic free-exciton emissions.

A. Temperature dependence of the interband transitions

The effects of temperature on the energy shift of interband transitions in the GaN samples were examined by both PL and PR measurements. Shown in Fig. 2 are PR spectra measured at different temperatures. The 20 K PR spectrum has three exciton resonances. The excitons referred to as the intrinsic A, B, and C exciton[7,8] are related to the $\Gamma_9^V-\Gamma_7^C$, Γ_7^V(upper band)$-\Gamma_7^C$, and Γ_7^V(lower band)$-\Gamma_7^C$ interband transitions in wurtzite GaN, respectively. The sharp derivative-like line shapes in PR spectra allow us to accurately determine the transition energies, particularly at high temperatures. The PR spectra were fitted to different line-shape functions. The solid lines in Fig. 2 are the best fits to the experimental data by the Lorentzian line-shape functional form[9–11]

$$\Delta R/R=\mathrm{Re}[Ce^{i\theta}(E-E_0+i\Gamma)^{-n}], \tag{1}$$

where C and θ are the amplitude and phase of the line shape, respectively, and E_0 and Γ are the energy and empirical broadening parameter of the transition, respectively. The exponent n is a characteristic parameter which depends on the type of critical point in the Brillouin zone and the order of

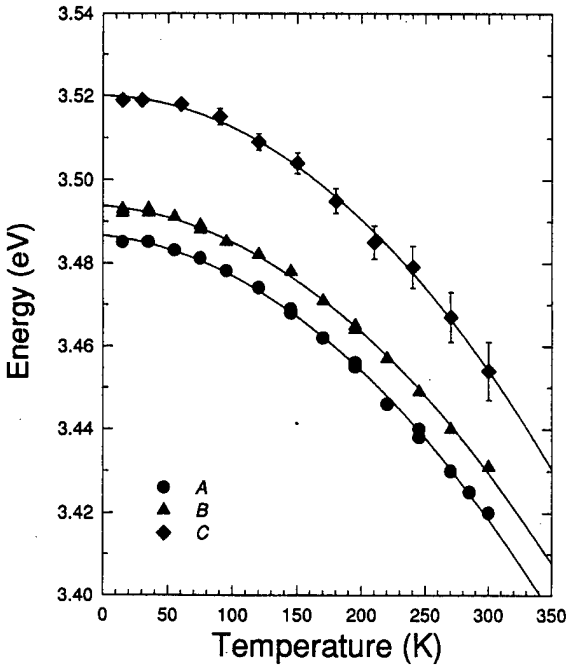

FIG. 3. Temperature dependence of three interband transition energies. $\Gamma_9^V-\Gamma_7^C$ transition: solid circles; Γ_7^V(upper band)$-\Gamma_7^C$ transition: solid triangles; and Γ_7^V(lower band)$-\Gamma_7^C$ transition, solid diamonds. The solid curves are least-squares fits to the experimental data using the Varshni empirical equation.

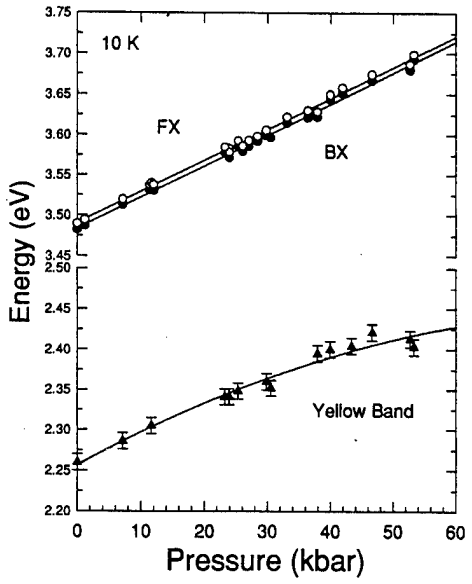

FIG. 4. Dependence of the energy positions on pressure for the various observed PL transitions in the GaN sample.

derivative. Both values of $n=2$ and $n=5/2$, which describe the nature of the interband excitonic transitions and three-dimensional band-to-band transitions, respectively, were used to fit the observed PR spectral structures. We found that using $n=2$ (corresponding to the first derivative line shape) results in a better fit to the line positions and widths of the PR spectra than using $n=5/2$ (the third derivative line shape). This was found to be appropiate even at the highest temperature employed. The best fits to the PR spectral features yield an energy of 3.420 eV for the lowest interband ($\Gamma_9^V-\Gamma_7^C$) transition and an energy of 3.428 eV for the second interband [Γ_7^V(upper band)$-\Gamma_7^C$] transition at room temperature (300 K), respectively.

Figure 3 plots the energies as a function of the temperature of all three observed interband excitonic transitions in the low-pressure MOCVD GaN. The temperature dependence for the interband transitions was deduced by using the Varshni empirical equation,[12]

$$E_0(T)=E_0(0)-\alpha T^2(\beta+T), \tag{2}$$

where $E_0(0)$ is the transition energy at 0 K, and α and β are constants referred to as Varshni thermal coefficients. The solid lines in the figure represent the least-squares fit to the experimental data using Eq. (2). The parameters obtained from the best fit are $E_0(0)=3.486$ eV, $\alpha=8.32\times10^{-4}$ eV/K, and $\beta=835.6$ K for the $\Gamma_9^V-T_7^C$ transition, and $E_0(0)=3.494$ eV, $\alpha=10.9\times10^{-4}$ eV/K, and $\beta=1194.7$ K for the Γ_7^V(upper band)$-\Gamma_7^C$ transition. Attempts to fit to Eq. (2) the Γ_7^V(lower band)$-\Gamma_7^C$ transition energies measured at different temperatures yield $E_0(0)=3.520$ eV, $\alpha=2.92\times10^{-3}$ eV/K, and $\beta=3698.9$ K. The values of α and β for the Γ_7^V(lower band)$-\Gamma_7^C$ transition are somewhat anomalously larger than those for the $\Gamma_9^V-\Gamma_7^C$ and Γ_7^V(upper band)$-\Gamma_7^C$ transitions. This is due primarily to the relatively large uncertainty in determination of the transition energy at high temperatures ($T>150$ K) caused by a poor signal-to-noise ratio.

B. Pressure coefficient and hydrostatic deformation potential for direct Γ band gap

In Fig. 4 we plot the peak energies of exciton emission and yellow emission structures measured by PL using the diamond-anvil cell as a function of pressure. The solid lines in the figure are the least-squares fits to the experimental data using the quadratic-fit function,

$$E(P)=E(0)+\alpha P+\beta P^2. \tag{3}$$

It is known that the emission lines associated with the radiative decay of a free exciton or a shallow bound exciton shift with the host semiconductor band gap under hydrostatic pressure at the same rate. The electron stays in the conduction-band-edge state or in the orbit of shallow donor state associated with the conduction-band edge. The excitonic hole bound in the Coulomb field retains the symmetry of the valence-band edges. Therefore, the change of the intense and sharp BX transition with pressure plotted in the figure provides an unmistakable signature of the direct Γ band-gap dependence for wurtzite GaN. The best fits to the data yield a linear slope of 3.86×10^{-3} eV/kbar with an extremely small sublinear term of -8×10^{-7} eV/kbar^2. Similar results can be obtained from fitting the FX transition as well ($\alpha=3.9\times10^{-3}$ eV/kbar and $\beta=-1.8\times10^{-6}$ eV/kbar^2).

The application of hydrostatic pressure, inducing a shift of the conduction-band edge relative to the valence-band edge due to a change in the volume, allows a direct estimation of the hydrostatic deformation potential for the direct Γ band gap of wurtzite GaN. The deformation potential is de-

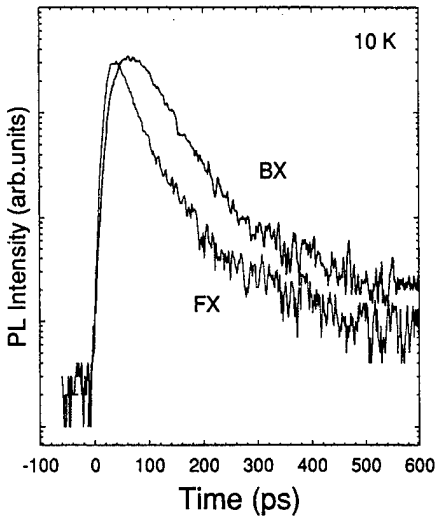

FIG. 5. Temporal variation of spectrally integrated PL for both intrinsic free and bound exciton emissions.

fined as $\mathbf{a}=\partial E/\partial \ln V$. The relative volume change caused by applied pressure can be related by the Murnaghan equation of state,[13]

$$P=(B_0/B_0')[(V_0/V)^{B_0'}-1], \tag{4}$$

where B_0 is the bulk modulus of the wurtzite GaN, B_0' is its pressure derivative ($=dB/dP$), V is the volume, and V_0 is the volume at atmospheric pressure. Using recently reported values of $B_0=2370\pm310$ kbar and $B_0'=4.3\pm2$,[14] the hydrostatic deformation potentials for the direct Γ band gap of wurtzite GaN could be deduced as $\mathbf{a}=-9.2\pm1.2$ eV.

The broad yellow emission band maximum was found to shift with pressure at a rate of 4.0×10^{-3} eV/kbar, almost the same as that of exciton emissions, but, it shows a relatively strong sublinear dependence compared to the exciton emissions. The broadband yellow emission spectral structure could be commonly observed in the PL spectra of nominally undoped GaN single crystals regardless of the crystal growth technique. More strikingly, this band was observed in samples implanted with a variety of atomic species.[15] These results have led to the general belief that the broadband emission in the yellow spectral region involves defects. Recent theoretical studies on the electronic structures of impurities and native defects in GaN have suggested that point defects, such as antisites and vacancies, play important roles.[16–19] The pressure dependence of the yellow emission band is consistent with the transitions involving shallow donors and deep acceptors because its pressure dependence follows the GaN band gap. Nevertheless, further theoretical and experimental studies are necessary to investigate the microscopic nature of the broadband yellow emission in GaN.

C. Radiative decay of free excitons and bound excitons

Temporal evolution of spectrally integrated exciton luminescence for both free exciton (FX) and bound exciton (BX) emissions observed in a GaN sample at 10 K is shown in Fig. 5. The overall time resolution of the experimental system used for conducting the measurements is less than 15 ps. The time evolution for both FX and BX luminescence is dominated by exponential decay. A much weaker long-decay component with an intensity more than two decades smaller compared to the main process could also be observed. The lifetime of the main PL decay was found to be ~35 ps for the FX emissions and ~55 ps for the BX emissions for the GaN sample at 10 K. It should be pointed out that the measurement of luminescence decay time does not provide a direct measurement of radiative lifetime. The measured PL decay time only yields an effective lifetime τ_{eff} for free excitons and bound excitons. It involves both the radiative τ_R and nonradiative τ_{NR} lifetimes with the decay rate expressed as

$$1/\tau_{\text{eff}}=1/\tau_R+1/\tau_{\text{NR}}. \tag{5}$$

The radiative lifetime for an excited state in a semiconductor can be estimated by considerations of optical transition probability. The radiative lifetime τ_R of the excited state can be described by[20,21]

$$\tau_R=2\pi\epsilon_0 m_0 c^3/\tilde{n}e^2\omega^2 f, \tag{6}$$

where f is the oscillator strength of the optical transition, $\tilde{n}$ is the refractive index, and the other symbols have their usual meanings. By using $\tilde{n}=2.4$ and $\omega\cong5.3\times10^{15}$ s^{-1} for GaN, one can roughly obtain $\tau_R\sim(800/f)$ ps. The radiative lifetime of bound excitons in GaN is expected to be just a little shorter than 1 ns and on the order of several hundreds of picoseconds if we take the upper limit with its oscillator strength as unity ($f\sim1$). The oscillator strength of free excitons calculated within the effective-mass approximation is given by $f=E_p/\pi\hbar\omega(V/a_x^3)$, where E_p is the Kane matrix element connecting Bloch states in the valence and conduction bands, V is the volume of unit cell, and a_x is the effective Bohr radius of free exciton. Our result yields $f\sim0.012$ for the free excitons in GaN using $E_p\sim18$ eV and $a_x\sim20$ Å. Thus, the calculated value of the radiative lifetime for free excitons in GaN will be in the domain of several tens of nanoseconds.

The discrepancy between the measured values of PL decay time and the theoretical estimated radiative lifetime can be attributed to nonradiative relaxation processes in competition with the radiative channel. In the case where nonradiative decay rate is larger, the measured decay time is characteristic for the nonradiative processes in accordance with Eq. (5). This situation is typical for recombination from intrinsic states of semiconductors. The nonradiative processes such as multiphonon emission, capture by deep centers, Auger effect, etc., give rise to fast relaxation of the excited carriers down to lower states from which they decay radiatively or relax nonradiatively. As a result, the measured PL decay time for a given excited state is an effective lifetime and usually much shorter than a radiative one. This has been observed in a number of semiconductor bulk materials and heterostructures with the measured free exciton PL decay time decreasing progressively as the density of nonradiative recombination centers increased. The slow rise of bound exciton luminescence intensity compared to that of the free exciton PL shown in Fig. 5 is an indicator of such nonradi-

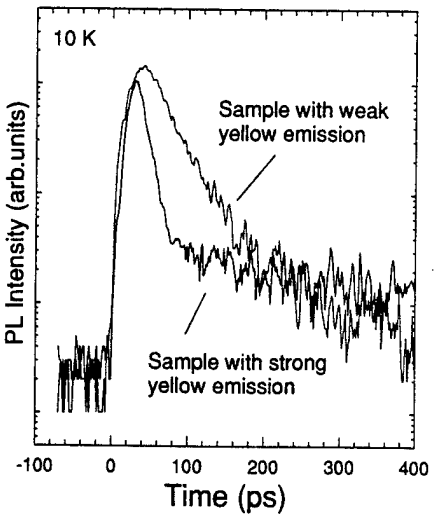

FIG. 6. Comparison of the time decay of free exciton emission between two GaN samples with the relative intensity ratio of 100:1 for the yellow emission under the same excitation conditions.

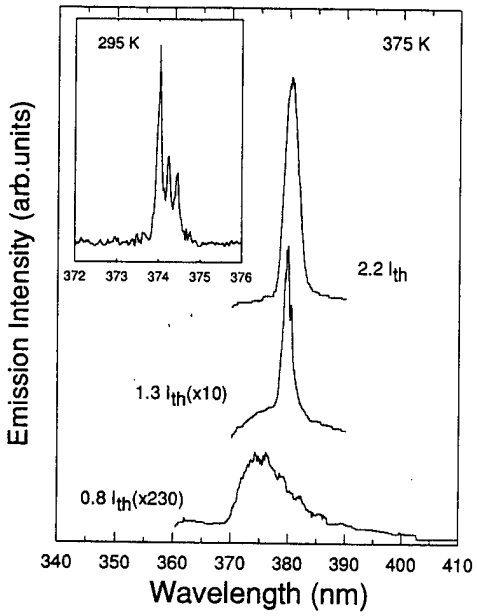

FIG. 7. Emission spectra of GaN at 375 K under different pumping power densities. The inset shows the longitudinal mode fringes.

ative relaxation processes for free excitons arriving at the bound exciton energy. We found that the capture of excitons and trapping of carriers by such nonradiative centers as defects and impurities play a major role in the recombination processes responsible for the exciton population decay in the GaN samples studied in this work. The measured PL decay time was found to be directly related to the intensity of broadband emissions lying in the GaN band gap. The broad emission structure referred to as yellow emission in the literature is believed to be associated with the optical transitions between the energy levels involving impurity and/or defect states. The intensity of yellow emission is proportional to the density of defects and impurities present in samples. We found that the stronger the yellow emission, the shorter the PL decay time in a GaN sample. Shown in Fig. 6 is a comparison of free exciton PL decay between two samples with the relative intensity ratio of 100:1 for the yellow emission under identical excitation conditions. The deduced lifetime of free exciton emission in the sample with stronger yellow emission is only 15 ps (which is the limit of our instrumental resolution). Therefore, the fast decay behavior of the PL intensity indicates that the capture of excitons and trapping of carriers at defects and impurities through nonradiative combinations dominate the decay of exciton population. The process of capture is dependent on the density of defects and impurities in the GaN samples.

D. Optically pumped stimulated emission and lasing

Strong stimulated emission and lasing at near-UV wavelengths could be observed from the GaN samples over a broad temperature range from 10 to over 400 K under the conditions of high-pumping power densities. In Fig. 7 we plot the emission spectra taken at 375 K for pumping power densities below and above the estimated threshold. Under low-excitation conditions, the spectrum is characterized by a very broad spontaneous emission band with the maximum positioning at 376 nm. With increasing pumping power densities, a second emission feature with a narrower line shape appears on the lower-energy side of the spontaneous emission band and becomes predominant as the pumping power densities are further increased. The emission feature is found to exhibit superlinear increase in intensity and a red shift of peak position as pumping power increases. In addition, the longitudinal cavity modes of lasing in some samples with small cavity lengths could clearly observed with a charge-coupled-device (CCD) camera. An example is given in the inset of Fig. 7, where the resonant cavity length of the sample is about 200 μm thick. The resonant cavity of the samples was prepared just by cutting the large wafer into barlike specimens with a diamond saw since it is almost impossible to cleave GaN grown on (0001) sapphire substrates. The resultant sample edges are far from mirrorlike facets.

The threshold pumping power was estimated to be ~500 kW/cm^2 at 10 K and ~800 kW/cm^2 at room temperature. Generally, the lasing threshold varies from sample to sample. For a given optical pumping source, the most important influence on the threshold is from the sample itself. This can be classified into two groups: One is associated with material properties, such as impurities, crystallinity, and defects; the other is related to the sample preparation, such as laser cavity length and the quality of sample edge facets. We expect that the value of the pumping power threshold for lasing in GaN can be lowered substantially by better preparing the sample facet edges, for example, with reflective coating. With better designed laser structures, such as double heterostructures, the lasing threshold is also expected to be significantly lowered. Recently, Zubrilov *et al.* reported the observation of multipass stimulated emission with Fabry–Pérot modes from GaN grown on 6H–SiC substrates.[6] In this case, the interference fringes originated from the microcavities. These cavities were formed by microcracks, which were generated during

the cleaving process. As better lattice-matched substrates become available for epitaxial growth of GaN with better crystallinity, the lasing threshold is expected to be lowered further.

We also note that the threshold is not very sensitive to the change of sample temperature. It is known that high-temperature sensitivity of the lasing threshold usually limits the performance of a laser under high-temperature operation.[22] The weak temperature dependence of the lasing threshold suggests that laser operation can be substantially extended to the high-temperature range. Thus, the results reported here imply that GaN-based laser diodes have the potential of operating with a much higher temperature tolerance compared to the conventional semiconductor laser diodes.

IV. CONCLUSIONS

We have employed a variety of experimental techniques to study the optical properties of GaN-grown sapphire by MOCVD. Optically pumped stimulated emission and lasing phenomena in GaN on sapphire were investigated using high-power pulsed lasers. Stimulated near-violet emissions were achieved with clearly observable longitudinal cavity modes over a wide temperature range from 10 up to 400 K. The dynamics of photoexcited excess carriers in high-quality GaN samples were investigated by transient luminescence spectroscopy in the picosecond regime using a streak camera in the region of near-band-edge excitonic emissions. We found that the strong capture of photoexcited carriers in impurities and/or defects through nonradiative recombination processes dominates the decay of carrier population. The capture process depends on the density of impurities and defects in the GaN samples. The effects of temperature and pressure on the various optical transitions associated with both intrinsic and extrinsic processes in the GaN samples were examined by photoluminescence and photoreflectance spectroscopy. The variation of the fundamental band gap of GaN was mapped out as a function of temperature. The room-temperature interband transition energy values obtained from these measurements are 3.420 eV for the $\Gamma_9^V-\Gamma_7^C$ transition and 3.428 eV for the Γ_7^V(upper band)$-\Gamma_7^C$ transition. By fitting the temperature-dependent energy values of the $\Gamma_9^V-\Gamma_7^C$ and Γ_7^V(upper band)$-\Gamma_7^C$ transitions to the Varshni empirical relation, our results yield

$$E_0(T)=3.486-8.32\times10^{-4}T^2/(835.6+T)\ \text{eV}$$

and

$$E_0(T)=3.494-10.9\times10^{-4}T^2/(1194.7+T)\ \text{eV},$$

respectively. The pressure coefficient of the GaN band gap was determined by studying the shift of exciton emission lines in GaN with applied pressure using the diamond-anvil pressure-cell technique. Our results yield the variation of GaN band gap with pressure to be

$$\Delta E(P)=3.9\times10^{-3}P-1.0\times10^{-6}P^2\ \text{eV}.$$

The deformation potential for the direct Γ band was also deduced from the experimental results to be -9.2 ± 1.2 eV.

ACKNOWLEDGMENTS

This work was supported by AFOSR, ARPA, ARO, and ONR. One of the authors (B.G.) is pleased to acknowledge the technical assistance of Maurice Hitchell.

[1] S. Strite and H. Morkoç, J. Vac. Sci. Technol. B **10**, 1237 (1992), and references therein.
[2] J. I. Pankove, Mater. Res. Soc. Symp. Proc. **162**, 515 (1990), and references therein.
[3] H. Morkoç, S. Strite, G. B. Gao, M. E. Lin, B. Sverdlov, and M. Burns, J. Appl. Phys. **76**, 1363 (1994), and references therein.
[4] S. Nakamura, Appl. Phys. Lett. **64**, 1687 (1994).
[5] X. H. Yang, T. Schmidt, W. Shan, J. J. Song, and B. Goldenberg, Appl. Phys. Lett. **66**, 1 (1995).
[6] A. S. Zubrilov, V. I. Nikovlaev, V. A. Dmitriev, K. G. Irvine, J. A. Edmond, and C. H. Carter, Jr., Inst. Phys. Conf. Ser. **141**, 525 (1995).
[7] B. Monemar, Phys. Rev. B **10**, 676 (1974).
[8] R. Dingle and M. Ilegems, Solid State Commun. **9**, 175 (1971).
[9] D. E. Aspnes, in *Optical Properties of Solids*, edited by M. Balkanski (North-Holland, Amsterdam, 1980), Chap. A.
[10] F. H. Pollak and O. J. Glembocki, Proc. SPIE **946**, 2 (1988).
[11] O. J. Glembocki and B. V. Shanabrook, in *Semiconductos and Semimetals*, edited by D. G. Seiler and C. L. Littler (Academic, San Diego, 1992), Chap. 4.
[12] Y. P. Varshni, Physica **34**, 149 (1967).
[13] F. D. Murnaghan, Proc. Nat. Acad. Sci. **30**, 244 (1944).
[14] M. Ueno, M. Yoshida, A. Onodera, O. Shimomura, and K. Takemura, Phys. Rev. B **49**, 14 (1994).
[15] J. I. Pankove and J. A. Hutchby, J. Appl. Phys. **47**, 5387 (1976).
[16] D. W. Jenkins and J. D. Dow, Phys. Rev. B **39**, 3317 (1989).
[17] T. L. Tansley and R. J. Egan, Phys. Rev. B **45**, 10 942 (1992); Physica B **185**, 190 (1993).
[18] J. Neugebauer and C. G. Van de Walle, Phys. Rev. B **50**, 8067 (1994).
[19] P. Boguslawski, E. Briggs, and J. Bernholc, Phys. Rev. B **51**, 17 255 (1995).
[20] D. L. Dexter, in *Solid State Physics*, edited by F. Seitz and D. Turnbull (Academic, New York, 1958), Vol. 6.
[21] G. W. 't Hooft, W. A. J. A. van der Poel, and L. W. Molenkamp, Phys. Rev. B **35**, 8281 (1987).
[22] G. P. Agrawal and N. K. Dutta, in *Semiconductor Lasers* (Van Nostrand Reinhold, New York, 1993), p. 132.

PROCEEDINGS REPRINT

SPIE—The International Society for Optical Engineering

Reprinted from

Physics and Simulation of Optoelectronic Devices IV

29 January–2 February 1996
San Jose, California

SPIE P PROCEEDINGS SERIES

Volume 2693

Invited Paper

Optical studies of epitaxial GaN based materials

J.J. Song, W. Shan, T. Schmidt, X.H. Yang, A. Fischer, S.J. Hwang, and B. Taheri
Center for Laser Research and Department of Physics, Oklahoma State University
Stillwater, OK 74078

B. Goldenberg and R. Horning
Honeywell Technology Center, Plymouth, MN 55441

A. Salvador, W. Kim, Ö. Aktas, A. Botchkarev, and H. Morkoç
Coordinated Science Laboratory, University of Illinois, Urbana, IL 61801

ABSTRACT

A variety of spectroscopic techniques has been used to study the optical properties of epitaxial GaN based materials grown by metalorganic chemical vapor deposition and molecular beam epitaxy. The emphasis was on the issues vital to device applications such as stimulated emission and laser action, as well as carrier relaxation dynamics. Sharp exciton structures were observed by optical absorption measurements above 300 K, providing direct evidence of the formation of excitons in GaN at temperatures higher than room temperature. Using a picosecond streak camera, the time decay of free and bound exciton emissions was studied. By optical pumping, stimulated emission and lasing were investigated over a wide temperature range up to 420 K. In addition, the optical nonlinearity of GaN was studied using wave mixing techniques.

1. INTRODUCTION

GaN based wide band-gap III-V nitride semiconductors currently attract much attention for their applications in electronic and optoelectronic devices, such as high power-high efficiency amplifiers, UV, blue, green, and yellow LED's, and in short-wavelength laser diodes.[1-3] With rapid progress in nitride epitaxial growth technology, high quality nitrides single crystal epifilms can now be grown on such substrates as sapphire and SiC. Recent demonstration of superbright high-efficient blue LED's, the development of the blue laser diode based on nitride heterostructures by the Nichia group[4,5] and the observation of optically pumped stimulated emission in GaN epifilms by a few groups[6,7] have led to increased interest in the development of efficient nitride UV-visible light emitters.

Although assessment of the properties and potential applications of nitrides is actively pursued to accelerate device fabrication, some vital issues directly related to optoelectronic device applications such as optically pumped stimulated emission and lasing, carrier dynamics, and optical nonlinearities have not been fully explored. In this report, we present the results of optical studies on the properties of GaN based epitaxial materials grown by metalorganic chemical vapor deposition (MOCVD) and molecular beam epitaxy (MBE) on sapphire substrates. Strong, sharp spectral structures associated with excitons in GaN based materials were observed in all samples used in this work by photoluminescence (PL) and

0-8194-2067-0/96/$6.00

optical absorption measurements. Optically pumped stimulated emission and lasing phenomena in GaN epitaxial layers and GaN/AlGaN heterostructures were investigated using high-power pulsed lasers. Stimulated emissions exhibiting longitudinal cavity modes were observed over a wide temperature range from 10 up to 420 K. The dynamics of photoexcited excess carriers in high quality GaN samples were investigated by transient luminescence spectroscopy in the picosecond regime using a streak camera in the region of near band-edge excitonic emissions. The nonlinear optical properties of GaN epitaxial layers were studied using degenerate four-wave mixing experiments. The nonlinear refractive coefficient of GaN was derived by examining the third order scattering efficiency.

2. EXPERIMENTAL DETAILS

The GaN samples used in this study were all nominally undoped single-crystal films grown on (0001) sapphire substrates by MOCVD. Thin AlN buffers of ~50 nm were deposited on sapphire substrates at 775°C before the growth of GaN. GaN layers were deposited at 1040°C directly on the AlN buffers. The GaN/AlGaN separate confinement heterostructures used in this work were grown on (0001) sapphire substrates by a modified reactive MBE at a substrate temperature near 800°C. The particular structure under discussion has a 600 Å thick AlN layer, directly grown on sapphire, followed by a GaN buffer layer, an AlGaN cladding layer, a lower mole fraction AlGaN waveguide layer, a 70 Å thick GaN quantum well, which is capped by a low mole fraction AlGaN waveguide, and an AlGaN cladding layer. The quantum well was doped with Si to a level of $5\times10^{17}cm^{-3}$.

Various optical measurements were carried out on the samples. Conventional photoluminescence (PL) spectra were measured with a cw HeCd laser (325 nm) as an excitation source and a 1-M double-grating monochromator connected to a photon-counting system. For optical absorption measurements, the quasi-monochromatic light dispersed by a ½-M monochromator from a halogen tungsten lamp was focused on the sample, and the transmission signals were detected using a lock-in amplifier system. Time-resolved photoluminescence (TRPL) measurements were performed using a frequency tunable pulsed laser (2 *ps* pulse duration, 82MHz) as an excitation source and a streak camera (2 *ps* resolution), in conjunction with a 1/4-M monochromator as a detection system. Stimulated emission and lasing experiments were carried out employing side-pumping geometry. A frequency-doubled pulsed Nd:YAG laser (532 nm) with a repetition rate of 10 Hz was used to pump a dye laser as a primary optical pumping source (10 *ns*). The output photon energy of the dye laser was then frequency doubled into UV wavelengths to photopump the GaN samples. The wave mixing experiments were performed using frequency doubled laser pulses (532 nm, 13 *ps*) from a mode-locked *Q*-switched Nd:YAG laser (10 Hz) in a forward propagating boxcar geometry.

3. RESULTS AND DISCUSSIONS

3.1 Exciton structures

The GaN samples studied in this work exhibit strong near-band-edge exciton luminescence. PL spectra taken from the samples are shown in Fig. 1. The strongest emission line marked by BX in the figure has a full width at half maximum (FWHM) of less than 1.0 *meV* at 10 K. The second one, labeled FX, shows a FWHM of less than 1.5 *meV*. The intensity of the BX peak was found to decrease much

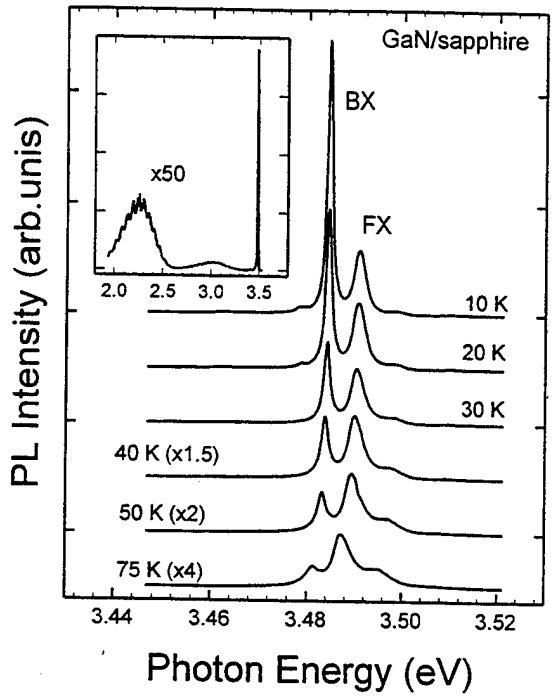

Fig. 1. Exciton luminescence spectra of a GaN sample taken at different temperatures. The inset shows the 10 K PL spectrum over a broad spectral range.

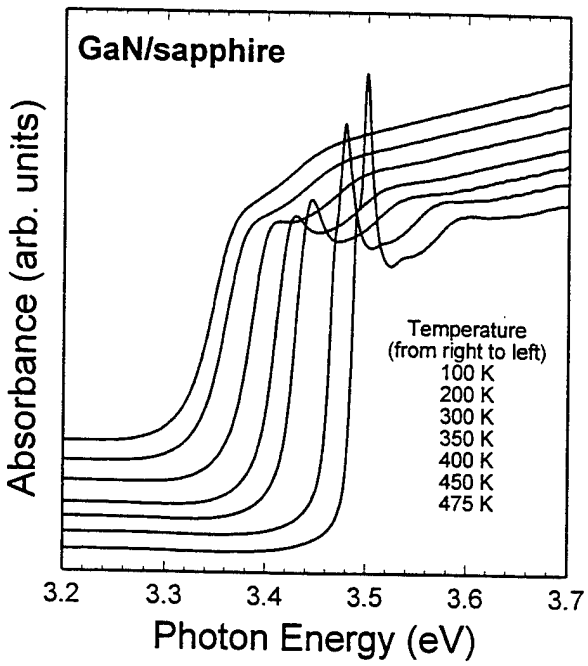

Fig. 2. Absorption spectra of a GaN epitaxial layer in the vicinity of fundamental absorption edge at different temperatures. The curves are vertically displaced for clarity.

faster than that of the FX as the temperature increased. It became hardly resolvable when the temperature was raised to above 100 K (not shown). Such variations of the luminescence intensity as a function of temperature indicate that the emission line can be attributed to the radiative recombination of excitons bound to neutral donors. The second strongest luminescence line, together with the weak emission feature on the higher energy side, can be assigned to intrinsic free-exciton emissions. The inset shows a broad range of the typical PL spectrum taken at 10 K. The broadband yellow emission and a weak emission band in the blue spectral region were observed.

Optical absorption measurements were performed on the GaN over a wide temperature range. The results for a thin GaN epitaxial layer in the vicinity of band edge at various temperatures are shown in Fig. 2. Sharp absorption peaks on the lower-energy side of the fundamental absorption edge are observed and are associated with the formation of excitons. Fine spectral features arising from the 1s state of the intrinsic free excitons associated with the split-off band edges of wurtzite GaN can be well resolved at low temperatures. The excitonic absorption resonance can be clearly observed well above room temperature up to higher than 400 K. Such clear observations of the excitonic absorption resonance above room temperature provide the direct evidence of the formation of excitons in GaN at temperatures higher than room temperature and indicate that the free exciton associated with the fundamental band gap of GaN has a substantially large binding energy. However, the complicated fundamental band edges of wurtzite GaN make it rather difficult to derive exciton binding energy unambiguously from the absorption spectra.

We also note that a weak absorption spectral feature is clearly visible in the energy region of

about 100 *meV* above the excitonic resonance. This is a real absorption structure though it is weaker and broader than the main absorption structures. It was also observed in photoreflectance, photoconductivity and photoluminescence excitation spectra taken from GaN epitaxial samples with various layer thicknesses grown on either sapphire or SiC substrates. Its temperature dependence is found to follow the main absorption edge, reminiscent of the transition from the third valence band (spin-orbit split-off band) to the conduction band in zinc-blende semiconductors. Unfortunately, there are few theoretical band structure calculations for wurtzite GaN detailing the band lineups in the vicinity of fundamental band gap for comparison. The identification of this transition requires further study.

3.2 Relaxation dynamics of free excitons and bound excitons

The temporal evolution of spectrally integrated exciton luminescence for both free-exciton (FX) and bound-exciton (BX) emissions observed in a GaN sample at 10 K is shown in Fig. 3. The overall time resolution of the experimental system used for conducting the measurements is less than 15 *ps*. The intrinsic free-exciton (FX) luminescence lines in these samples can be spectrally well resolved from that of excitons bound to neutral donors, as shown in the inset in the figure. That allows an unambiguous determination of the PL decay time for both intrinsic free excitons and neutral-donor bound excitons. The lifetime of the PL decay at 10 K was found to be typically about 35 ± 5 *ps* for free excitons and 45-55 *ps* for bound excitons, varying from sample to sample used in this work. The measured decay time is much shorter than the value estimated by theoretical considerations regarding the radiative lifetime of an excited state in a semiconductor, where the radiative lifetime of bound excitons in GaN is expected to be on the order of several hundreds of picoseconds and that of free excitons in the nanosecond domain.[8]

The discrepancy between the measured values of PL decay times and the theoretical estimated ones can be attributed to nonradiative relaxation processes in competition with the radiative channel. The measured PL decay time only yields an effective lifetime (τ_{eff}) for free excitons and bound excitons. It is related to both the radiative (τ_R) and nonradiative (τ_{NR}) lifetimes with the decay rate expressed as

$$1/\tau_{eff}=1/\tau_R+1/\tau_{NR}. \qquad (1)$$

In this equation, we have assumed that the nonradiative decay is exponential so that a lifetime can be defined, and that the carriers in the levels which undergo recombination are at thermal equilibrium. When the nonradiative decay rate is larger, the measured decay time is characteristic for the nonradiative processes in accordance with Eq.(1).

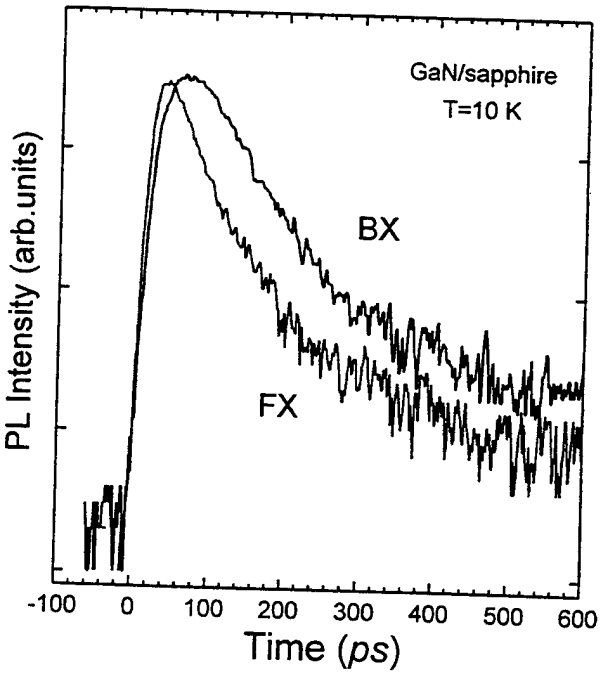

Fig. 3. Temporal evolution of spectrally integrated PL for both intrinsic free-exciton and bound-exciton emissions in a GaN sample at 10 K.

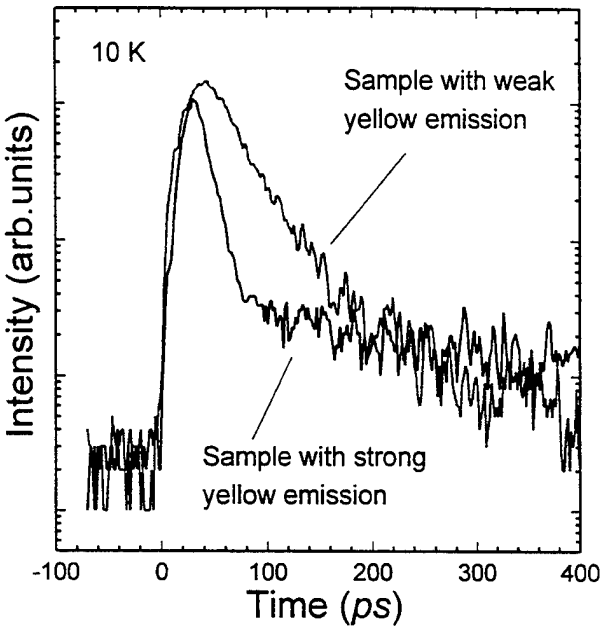

Fig. 4. Comparison of the time decay of free-exciton emission between two GaN samples with the relative intensity ratio of 100:1 for the broadband yellow emission under the same excitation conditions.

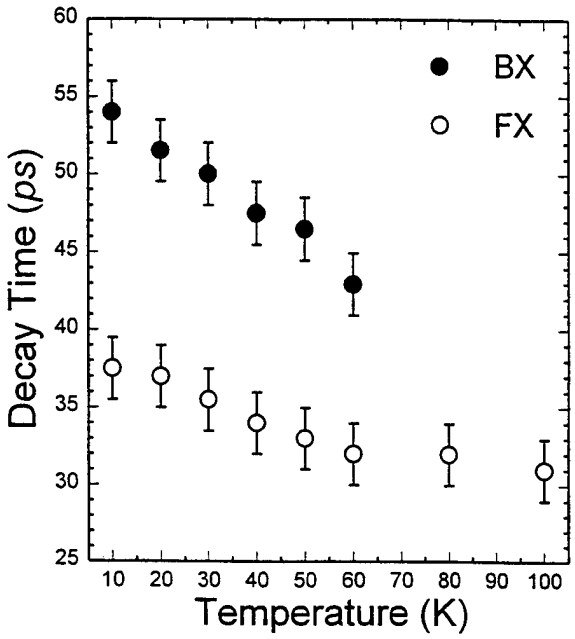

Fig. 5. The measured decay times for free-exciton emission and bound-exciton emission as a function of temperature.

This situation is typical for recombination from intrinsic states of semiconductors.[9] The nonradiative processes, such as multiphonon emission, capture by deep centers, Auger effect, *etc.*, give rise to fast relaxation of the excited carriers down to lower states from which they decay radiatively or relax nonradiatively. As a result, the measured PL decay time for a given excited state is an effective lifetime and usually much shorter than a radiative one. The slow rise of bound-exciton luminescence intensity compared to that of the free-exciton PL shown in Fig. 3 is an indicator of such nonradiative relaxation processes for free excitons arriving at the bound exciton energy. Therefore, the capture of excitons and trapping of carriers by such nonradiative centers at defects and impurities must play a major role in the recombination processes responsible for the exciton population decay in the GaN samples studied in this work. In fact, the measured PL decay time was found to be directly related to the intensity of broadband emissions lying in the GaN band gap. The broad emission structure referred to as yellow emission in the literature is believed to be associated with the optical transitions between the energy levels involving impurity and/or defect states. The intensity of yellow emission is proportional to the density of some particular defects or impurities present in samples. We found that the stronger the yellow emission, the shorter the PL decay time in a GaN sample. Fig. 4 compares free-exciton PL decay between two samples with the relative intensity ratio of *100:1* for the yellow emission under identical excitation conditions. The deduced lifetime of free-exciton emission in the sample with stronger yellow emission is only 15 *ps* (which is the limit of our instrumental resolution). Therefore, the fast decay behavior of the intensity indicates that the capture of excitons and trapping of carriers at defects and impurities through nonradiative combinations dominate the decay of the exciton population.The process of capture, therefore, must depend on the density of defects and impurities in the GaN samples.

The influence of nonradiative recombination on the measured decay time of exciton luminescence

can be further manifested by the effects of sample temperature. It is known that for a radiative recombination dominant system, an increase in the radiative lifetime with temperature is expected for the free excitons[10,11] since their average kinetic energy is increased. The thermal redistribution results in a decreasing number of the excitons close enough to the Brillouin-zone center for radiative recombination. Also the lifetime is expected to be independent of temperature for bound excitons, and only the emission intensity is expected to decrease because of thermal ionization of the bound excitons. However, the bound-exciton PL decay time was found to decrease with increasing temperature before the emission thermally quenched, and the free-exciton PL decay time measured from the majority of samples used in this work exhibited a slow decrease with temperature, as shown in Fig. 5. Although recombination from excitons bound to extrinsic states such as defects or impurities can often be very efficient at low temperatures as demonstrated by Fig. 1, the measured decay time is still determined by detailed decay kinetics. The observed decrease of PL decay time with temperature for the bound excitons in the GaN samples indicates that incrementally stronger nonradiative relaxations occur as the temperature increases, resulting in continued faster decay of the exciton population. The decrease of free-exciton PL in both intensity and decay time with temperature suggests that the nonradiative processes of capture of free excitons at defects or impurities prevail in the competition with the thermally enhanced exciton-exciton and exciton-phonon scatterings.

3.3 Optically pumped stimulated emission and lasing

With a carefully designed optical pumping scheme, optically pumped stimulated emission and laser actions were achieved in the GaN samples with bar-like shape under both picosecond and nanosecond laser excitations. The laser actions could be observed over a broad temperature range from 10 K up to 400 K. All samples exhibit, more or less, longitudinal lasing modes in their emission spectra. Fig. 6 plots the emission intensity against the pumping power density. The observations of superlinear increase in intensity with the excitation power density, together with the spectral narrowing and the complete suppression of the broad emission background, are typical characteristics of the occurrence of stimulated emission. The onset of the superlinear increase in emission intensity is defined as the lasing threshold. The threshold was found to be weakly dependent on temperature. Our results yield a factor of less than two for the increase in the threshold, from $\sim 500\ kW/cm^2$ at 10 K to $\sim 800\ kW/cm^2$ at room temperature (295 K).

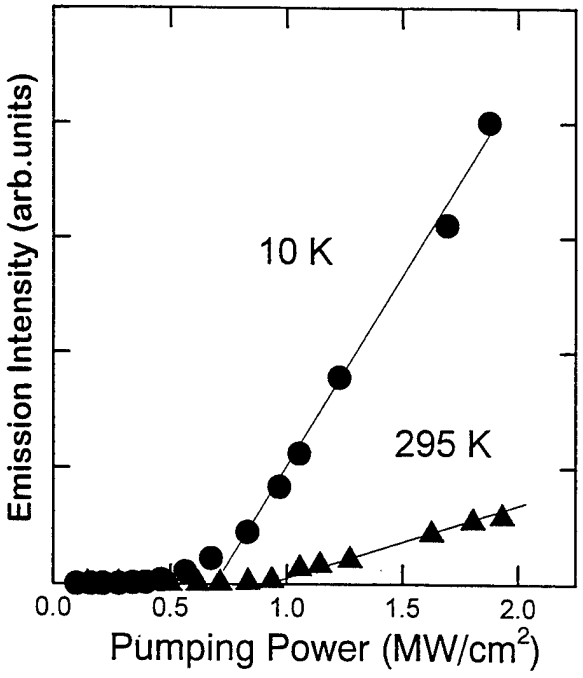

Fig. 6. Measured emission output vs. Pumping power density at 10 K and room temperature (295 K). The onset of the superlinear increase in emission intensity is defined as the lasing threshold.

Generally, the threshold value can be affected by parameters that are dependent on the pumping source and sample. For a given optical

pumping source, the most important influence on the threshold is from the sample itself with the threshold varying from sample to sample. This can be classified into two groups: one is associated with material properties, such as impurities, crystallinity, and defects; the other is related to the sample preparation, such as laser cavity length and the quality of sample edge facets. We expect that the value of the pumping power threshold for lasing in GaN can be lowered substantially by better preparing the sample facet edges, for example, with reflective coating. With the crystalline quality further improved and better designed laser structures for carrier confinement and waveguiding, such as double heterostructures or quantum well structures being used, the lasing threshold is also expected to be significantly lowered.

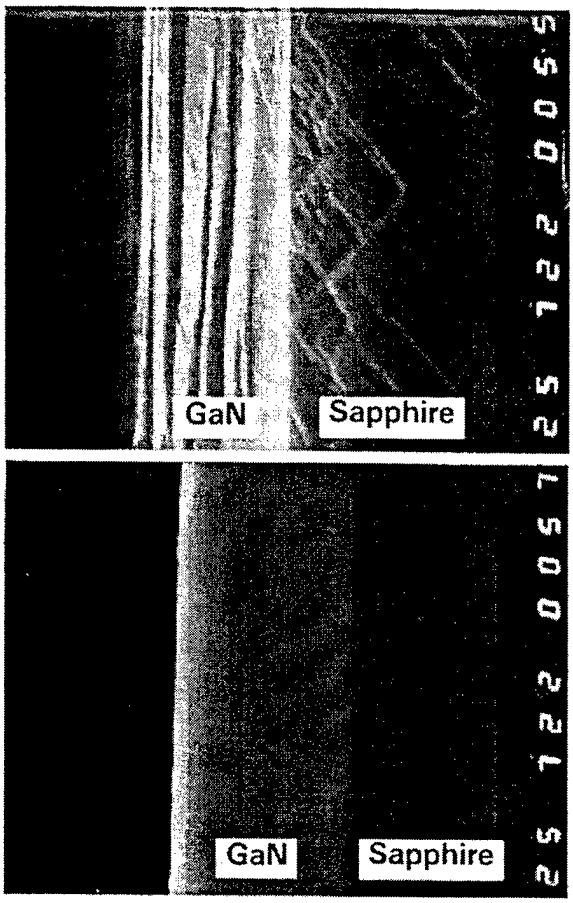

Fig. 7. Images of the surface morphology of GaN layers: cutting facet without polishing (upper portion) and fine polished facet (lower portion). The photographs were taken by SEM.

The specimens used in this optical pumping experiment were bar-like pieces merely cut off rather than cleaved from the large GaN wafer due to the well-known difficulties of forming high quality facets in sapphire. However, with attempts to finesse the cut surfaces, as shown in Fig. 7, we did observe some substantial improvements in terms of Fabry-Perot cavity mode fringes. Fig. 8 shows a comparison of three lasing spectra taken under almost the same pumping conditions from three specimens subjected to different treatments and demonstrates the progressive improvement of the quality of observed mode fringes. The spectrum exhibited line-width narrowing and mode fringes enhancing, after the specimen's facet edges were fine polished. When a set of external mirrored cavity was imposed to the samples, the mode quality was much improved. In addition, the emission intensity was found to increase by a factor of two.

We have also performed optical gain measurements using the approach of monitoring the emission intensity at fixed power levels by varying the length of the excitation beam on an as-cut sample. Fig. 9 plots the emission intensity as a function of excitation length at selected pumping power levels. The measured gain values are also given in the figure, which are within the range of recently published theoretical calculation results.[12,13]

The significant reduction of room-temperature threshold has been recently observed in MBE GaN/AlGaN separate confinement heterostructure (SCH) samples. The pumping threshold for stimulated emission was determined to be $\sim 90\ kW/cm^2$, approximately one order of magnitude less than the value

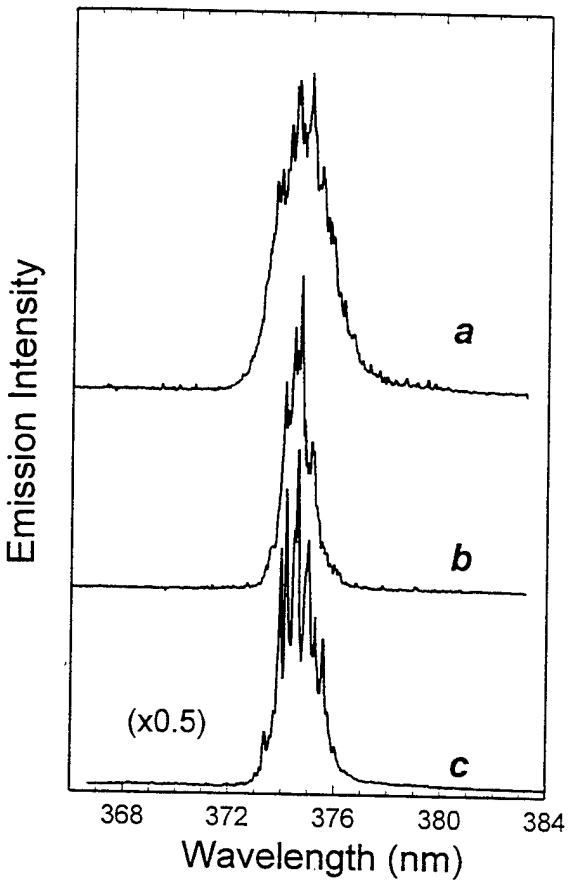

Fig. 8. Comparison of lasing spectra taken at 295 K under almost the same excitation conditions from three samples subjected to progressive treatments: (a) simply cut from wafer; (b) facet surface fine polished; (c) external mirror cavity imposed.

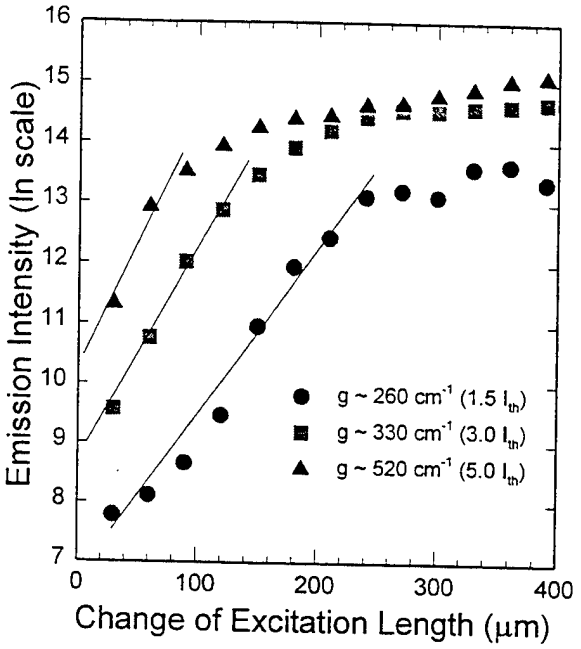

Fig. 9. The variation of emission intensity with the excitation beam length on an as-cut sample surface at selected pumping power levels at 295 K. The estimated optical gain values for the GaN sample are given in the figure. The pumping threshold $\mathbf{I}_{th}$=800 *kW/cm²*.

for the GaN epitaxial bulk given above even though the SCH sample edges were not cut parallel to each other. The substantial decrease in the stimulated emission threshold can be attributed to the carrier confinement and waveguiding effects of the SCH structure. Detailed discussions of the results will be reported elsewhere.[14] It should be noted here that the specimens used in this optical pumping experiment were small pieces simply cut off from the large GaN/AlGaN SCH wafer with no attempt to finesse the cut surfaces. This provides a basis for our optimism that the pumping power threshold for stimulated emission and lasing in these samples can be further reduced with improved facets.

3.4 Picosecond degenerate four-wave mixing at 532 nm

The degenerate wave mixing experiments were performed using frequency-doubled pulses from a mode-locked, Q-switched Nd:YAG laser operating with a repetition rate of 10 Hz. The 532 nm pulse (13 *ps*) has a quasi-Gaussian spatial and temporal profile. The second harmonic output of the laser was equally split in energy into two pump beams and one probe beam. These beams were spatially and temporally recombined in the samples in a forward propagating boxcar geometry.[15] The two pump beams were σ-polarized, while the probe beam was π-polarized in order to increase the signal-to-noise ratio and minimize interactions between the pump and probe beams. An energy meter preceded by a polarizer was used to detect the π-polarized diffracted signal. At the front surface of the sample, the two pump beams

have a small crossing angle (2θ). The probe was incident on the interference region at a small angle with respect to the plane of the pump beams. In such a wave-mixing geometry, the pump beams set up an interference pattern in their overlap region with fringe spacing $\Lambda = \lambda/2\sin\theta$, where λ is the wavelength of the beams in free space. Intensity dependence causes the index of refraction in the light regions of the interference pattern to differ from that in the dark region. The overlap region, therefore, behaves as an index grating with spacing of Λ. An incident probe beam will be diffracted from this grating in the directions satisfied by the phase matching conditions. Fig. 10 shows a photograph of the diffracted signals together with the three attenuated incident beams when they are temporally overlapped in a thick GaN sample. The picture was taken at room temperature with the pump beam focal spot of $\sim 500\ \mu m$ and the probe beam of $\sim 400\ \mu m$ and total incident irradiance of 1.7 GW/cm^2. The clearly visible patterned spots are diffracted higher order wave-mixing signals in the phase-matching directions. The strong diffracted signals in this wide band-gap material are consistent with the elegant band charge model, which predicts higher nonlinearities as the material becomes more polar.[16-18]

By delaying the arrival of the probe pulses relative to the pump pulses, the response of the nonlinear optical changes such as scattering efficiency in the GaN sample was studied. The scattering efficiency is defined as the ratio of the intensity of scattered to the transmitted probe beam. Scattering efficiency for an index grating can be expressed as:[15]

$$\eta(t) = I_{\text{scattered}} / I_{\text{transmitted}} = \sin^2\{k\Delta n(t) l/2\} \approx \{k\Delta n(t) l/2\}^2, \qquad (2)$$

where k is the wave vector of the probe beam, $\Delta n(t)$ is the time dependent index change and l is the sample thickness. Fig. 11 illustrates the change of scattering efficiency as a function of the time delay of the probe beam. The non-exponential temporal evolution of the scattering efficiency is primarily caused

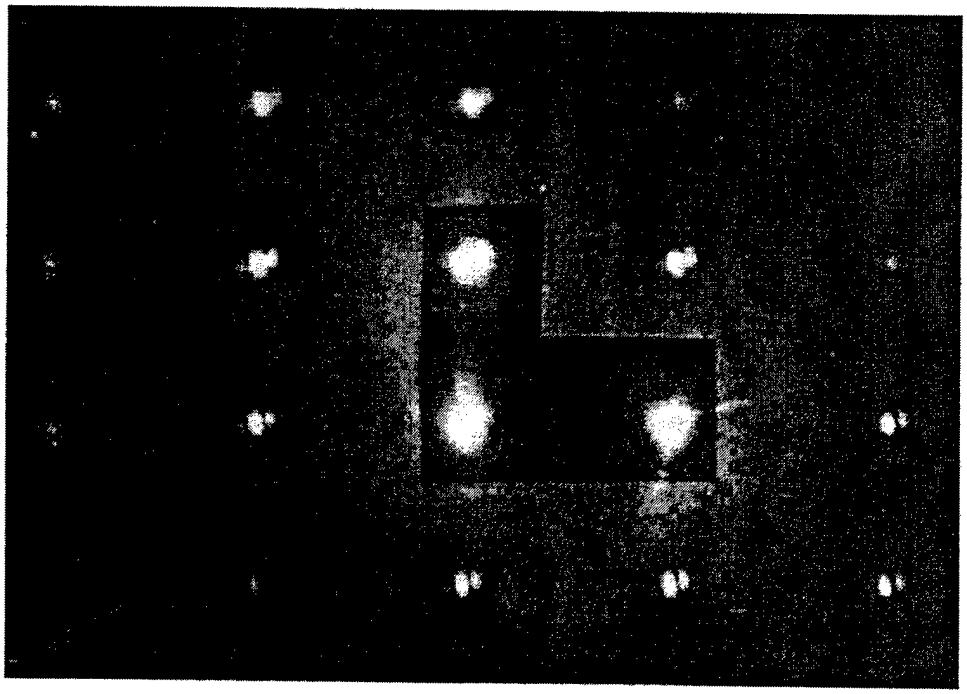

Fig. 10. Photograph of the wave mixing signals showing three attenuated pump and probe beams and higher order nonlinear diffracted signal spots. The laser photon energy (2.33 *eV*) is well below the room-temperature GaN band gap (3.42 *eV*).

by the decay of the pump-induced refractive index grating due to the combined effects of both recombination and diffusion of excited carriers. At zero delay, a maximum scattering efficiency of 4×10^{-5} was obtained. It corresponds to an index change, $\Delta n(0)$, of 1.2×10^{-3}. This change can be related to the pump beam intensity through an effective nonlinear refractive coefficient, n_2, defined as

$$\Delta n(0)=n_2 I_0. \qquad (3)$$

Provided the pump-beam irradiance of 1.2 GW/cm^2, a value of 1×10^{-3} cm^2/GW was derived for the effective nonlinear refractive index n_2 from Eq.(3). Compared to the value of other wide band-gap semiconductor materials, for instance, 6.7×10^{-5} cm^2/GW for ZnSe,[19] it is more than an order of magnitude higher, indicating the large optical nonlinearities for GaN.

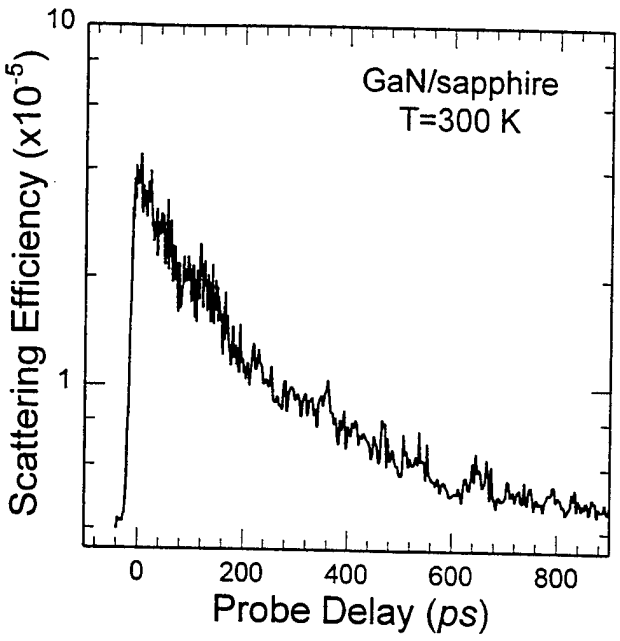

Fig. 11. Scattering efficiency measured as a function of the time delay of probe pulse. A maximum refractive index change can be derived from the result at zero delay.

4. CONCLUSIONS

Strong, sharp spectral structures associated with excitons in epitaxial GaN based materials were observed in photoluminescence and optical absorption spectra over a wide temperature range. In particular, the observation of sharp absorption peaks at the lower energy side of the absorption edge above room temperature provided direct evidence of the formation of excitons in GaN at high temperatures (>300 K). The relaxation dynamics of photoexcited carriers in GaN were studied by examining the radiative decay of exciton emissions using time-resolved photoluminescence spectroscopy. We found that the capture of excitons and trapping of carriers at defects and/or impurities through nonradiative relaxation processes dominate the decay of exciton population, resulting in a very short decay time for both free-exciton and bound-exciton emissions. The capture process depends on the density of impurities and defects in the GaN samples. Optically pumped stimulated emission and lasing phenomena in GaN and AlGaN/GaN heterostructures were investigated using high-power pulsed lasers. Stimulated emission and laser action were observed over a wide temperature range from 10 K to ~420 K. The pumping power threshold for lasing was estimated as ~500 kW/cm^2 at 10 K to ~800 kW/cm^2 at 295 K for bulk GaN epitaxial samples. The MBE grown GaN/AlGaN SCH samples were found to exhibit stimulated emission threshold pumping powers as low as 90 kW/cm^2 at room temperature. This represents an order of magnitude reduction over the bulk GaN. The results suggest that the carrier confinement and waveguiding effects of the SCH samples give rise to a substantial decrease in the stimulated emission threshold. In addition, we found that the lasing mode quality can be substantially improved by finessing the cut facet edges of GaN on sapphire substrates. Strong high order nonlinear diffraction signals of

degenerate four-wave mixing were found in GaN epitaxial layers in three-beam forward propagating boxcar geometry. The nonlinear refractive index at 532 nm was determined for GaN by the measurement of maximum absolute scattering efficiency using picosecond wave mixing technique.

5. ACKNOWLEDGMENTS

This work at OSU was supported by AFOSR, ARPA, ONR and ARO. The work at UIUC was supported by grants from ONR, AFOSR, and BMDO. H.M. is funded by a university president research program funded by AFOSR. B.G. is pleased to acknowledge the technical assistance of Maurice Hitchell.

6. REFERENCES

1. S. Strite and H. Morkoç, J. Vac. Sci. Technol. **B10**, 1237(1992), and references therein.
2. J.I. Pankove, Mater. Res. Soc. Symp. Proc. **162**, 515(1990), and references therein.
3. H. Morkoç, S. Strite, G.B. Gao, M.E. Lin, B. Sverdlov, and M. Burns, J. Appl. Phys. **76**, 1363(1994).
4. See, for example, S. Nakamura, J. Vac. Sci. Technol. **A13**, 705(1995).
5. S. Nakamura, M. Senoh, S. Nagahama, N. Iwasa, T. Yamada, T. Matsushita, H. Kiyoku, and Y. Sugimoto, Jpn. J. Appl. Phys. **35**, part.2, Jan. 15 (1996).
6. X.H. Yang, T. Schmidt, W. Shan, J.J. Song, and B. Goldenberg, Appl. Phys. Lett. **66**, 1(1995).
7. A.S. Zubrilov, V.I. Nikovlaev, V.A. Dmitriev, K.G. Irvine, J.A. Edmond, and C.H. Carter, Jr., Inst. Phys. Conf. Ser. No.141, 525(1995).
8. W. Shan, X.C. Xie, J.J. Song, and B. Goldenberg, Appl. Phys. Lett. **67**, 2512(1995).
9. M. Voos, R.F. Leheny, and J. Shah, in *Optical Properties of Solids*, edited by M. Balkanski, (North-Holland, Amsterdam, 1980), Chapter 6, p.336.
10. J. Feldmann, G. Peter, E.O. Göbel, P. Dawson, K. Moore, C. Foxon, and R.J. Elliott, Phys. Rev. Lett. **59**, 2337(1987).
11. G.W. 't Hooft, W.A.J.A. van der Poel, and L.W. Molenkamp, Phys. Rev. **B35**, 8281(1987).
12. W. Fang and S.L. Chuang, Appl. Phys. Lett. **67**, 751(1995).
13. W.W. Chow, A. Knorr, and S.W. Koch, Appl. Phys. Lett. **67**, 754(1995).
14. T.J. Schmidt, X.H. Yang, W. Shan, J.J. Song, A. Salvador, W. Kim, Ö. Aktas, A. Botchkarev, and H. Morkoç, to be published in J. Appl. Phys.
15. H.J. Eichler, P. Gunter, and D.W. Pohl, *Laser-Induced Dynamic Gratings*, (Springer-Verlag, Berlin, 1986), p.47.
16. C.L. Tang and C. Flytzanis, Phys. Rev. **B4**, 2520(1971).
17. B.F. Levine, Phys. Rev. **B7**, 2600(1973).
18. F.W. Scholl and C.L. Tang, Phys. Rev. **B8**, 4607(1973).
19. M. Sheik-Bahae, A.A. Said, T.H. Wei, D.J. Hagan, and E.W. van Stryland, IEEE J. Quantum Electron. **26**, 760(1990).

Optical studies of GaN and GaN/AlGaN heterostructures on SiC substrates

W. Shan,[a] A. J. Fischer, and J. J. Song
Center for Laser Research and Department of Physics, Oklahoma State University, Stillwater, Oklahoma 74078

G. E. Bulman, H. S. Kong, and M. T. Leonard
Cree Research, Inc., Durham, North Carolina 27713

W. G. Perry, M. D. Bremser, and R. F. Davis
Department of Materials Science and Engineering, North Carolina State University, Raleigh, North Carolina 27695

(Received 22 April 1996; accepted for publication 29 May 1996)

We present the results of spectroscopic studies on GaN based epitaxial materials on SiC substrates by metalorganic chemical vapor deposition. A variety of techniques has been used to study the optical properties of GaN epilayers and GaN/AlGaN heterostructures. Sharp spectral structures associated with the intrinsic free excitons were observed by photoluminescence and reflectance measurements from GaN based materials grown on SiC substrates. The residual strain was found to have a strong influence in determining the energies of exciton transitions. Picosecond relaxation studies of exciton decay dynamics suggest that an AlGaN cladding layer with a small mole fraction of AlN can be relatively effective in enhancing the radiative recombination rate for excitons by reducing the density of dislocations and suppressing surface recombination velocity in the GaN active layer for the GaN/AlGaN heterostructure samples. © *1996 American Institute of Physics.* [S0003-6951(96)04532-9]

GaN based wide band-gap III–V nitride semiconductors have been extensively studied for their device applications, such as high-power amplifiers, UV, blue, green, and yellow light-emitting diodes (LED's), and short-wavelength laser diodes.[1–3] Observation of optically pumped stimulated emission in GaN epifilms has led to increased interest in the development of efficient nitride UV-visible light emitters.[4,5] In fact, superbright high-efficiency blue LED's have recently been commercialized and current-injection laser diodes based on nitride heterostructures have been reported by the Nichia group.[6,7] So far, the majority of research activities, including the assessment of material properties and the development of devices, has concentrated on nitrides grown on sapphire substrates, although its lattice parameter and coefficient of thermal expansion are significantly different from that of any III nitrides. An alternative substrate material for III-nitride epitaxial growth is SiC. It has many advantages over sapphire in terms of nitride epitaxy deposition and device fabrication: close match of lattice parameters and coefficient of thermal expansion to that of III nitrides; higher thermal conductivity of SiC offers greater power handling and improved reliability; and both *n*- and *p*-type electrical conductivity can be achieved allowing vertical device structure. In this report, we present the results of optical studies of the properties of GaN epilayers and GaN/AlGaN heterostructures grown by metalorganic chemical vapor deposition (MOCVD) on 6H–SiC (0001) substrates. The effects of strain on the exciton transitions in the GaN epitaxial materials on SiC were examined and compared with those observed in the GaN epilayer on sapphire samples. The dynamics of photoexcited excess carriers in the region of near-band-edge excitonic emissions were investigated by transient luminescence spectroscopy in the picosecond regime.

Samples used in this study were all nominally undoped single-crystal films grown on (0001) 6H–SiC substrates by MOCVD. AlN buffers were deposited on the substrates before the growth of GaN. GaN layers were deposited at 1050 °C directly on the AlN buffers. The GaN/AlGaN heterostructures used in this work included both double heterostructure (DH) samples and separate confinement heterostructure (SCH) samples. The DH and SCH structures were deposited on GaN epilayers with the thickness typically around three microns. The particular DH structure under discussion has an ~800 Å thick GaN active layer, surrounded by a few thousand Å $Al_{0.1}Ga_{0.9}N$ cladding layers. The SCH structure consists of a 100 Å thick GaN quantum well, with an $Al_xGa_{1-x}N$ cladding layer and a lower mole fraction $Al_xGa_{1-x}N$ waveguide layer symmetrically locating on each side. The nominal Al compositions are 11% and 6%, respectively. Conventional photoluminescence (PL) spectra were measured with either a cw HeCd laser (325 nm) or a frequency-doubled Ar^+ laser (244 nm) as the excitation source and a 1-M double-grating monochromator connected to a photon-counting system. For reflectance measurements, the quasimonochromatic light dispersed by a $\frac{1}{2}$-M monochromator from a xenon lamp was focused on the sample, and the reflectance signals were detected using a lock-in amplification system. Time-resolved photoluminescence (TRPL) measurements were performed using a frequency tunable pulsed laser (2 ps pulse duration, 76 MHz) as an excitation source and a streak camera (2 ps resolution), in conjunction with a $\frac{1}{4}$-M monochromator as a detection system.

The GaN based samples studied in this work exhibit strong near-band-edge exciton luminescence. Results of PL spectroscopy from a 3.7-μm GaN epilayer sample are shown in Fig. 1 at selected temperatures. The intensity of the strongest emission line marked by BX in Fig. 1 was found to decrease much faster than that labeled FX as the temperature

[a]Electronic mail: wshan@osuunx.ucc.okstate.edu

 0003-6951/96/69(6)/740/3/$10.00

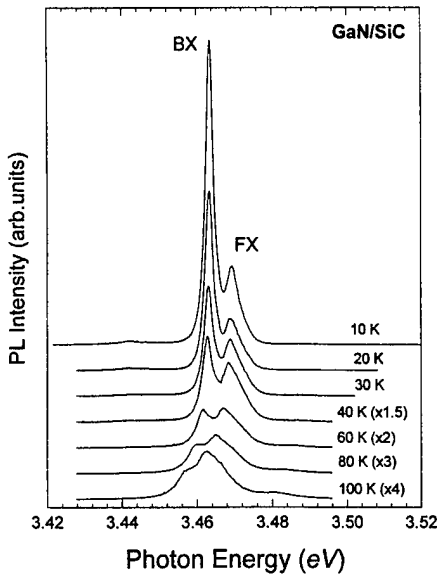

FIG. 1. Near-band-edge exciton luminescence spectra taken from a 3.7-μm GaN epilayer on SiC at selected temperatures.

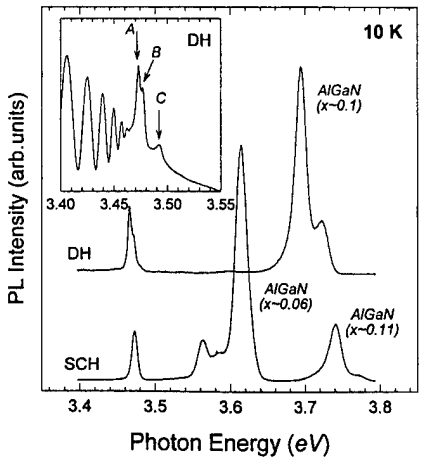

FIG. 3. 10-K PL spectra of a DH and a SCH sample grown on SiC. The inset illustrates the exciton transition signatures of the GaN active layer in the DH sample measured by reflectance spectroscopy.

increased. It became hardly resolvable at the temperatures higher than 100 K (not shown). Such variations of the luminescence intensity as a function of temperature indicate that the emission line can be attributed to the radiative recombination of excitons bound to neutral donors. The second strongest luminescence structure, together with the weak emission feature on the higher energy side, can be assigned to intrinsic free-exciton emissions. Figure 2 shows a reflectance spectrum taken from the sample at 10 K. Three exciton resonances associated with the transitions referred to as the *A*, *B*, and *C* exciton transitions[8,9] between the bottom of the conduction band (Γ_7^C) and three topmost valence band edges ($\Gamma_9^V+\Gamma_7^V+\Gamma_7^V$) are indicated by vertical arrows. The energy positions of these transitions are 3.470, 3.474, and 3.491 eV, respectively. We note that the values of the transition energies obtained here are lower than those reported in the literature,[9–11] for example, 3.485, 3.493, and 3.518 eV, for GaN on sapphire substrates.[10] Such discrepancy can be attributed to the effects of residual strain in the epilayers due to the mismatch of lattice parameters and coefficients of thermal expansion between GaN and the substrate materials.[11,12] Because of the inevitable occurrence of strain relaxation by the formation of a large density of dislocations, it is generally difficult to separate the strain effects caused by lattice-parameter mismatch from the ones involving thermal-expansion mismatch so as to exactly determine their influences on the optical properties of GaN epitaxial layers. However, by comparing the observed exciton transition energies in GaN epilayers deposited on sapphire and SiC to the values (3.4751, 3.4815, and 3.503 eV) obtained from virtually strain-free bulk GaN reported in Ref. 9, one can infer that the overall effects of residual strain generated in GaN on sapphire is compressive, which results in an increased band gap, while the stress induced in GaN on SiC is tensile, which leads to a decrease in measured exciton transition energies. Therefore, we conclude that residual strain induced by thermal-expansion mismatch in GaN based epitaxial layers has the prevailing influence on the energy variations of exciton transitions, since lattice-mismatch induced strain has a completely opposite effect on the variation of the GaN band gap.

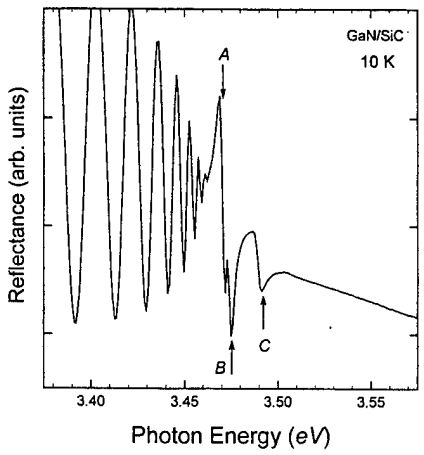

FIG. 2. Reflectance spectrum of the exciton transition region of the MOCVD GaN/SiC sample at 10 K. The oscillatory structures at lower energy are interference effects caused by the heterointerface.

Figure 3 shows the 10 K PL spectra of the DH and SCH samples. The inset highlights the signatures of intrinsic free exciton transitions observed by reflectance measurements from the GaN active layer of the DH structure. The emission peaks at the energy position around 3.47 eV in the PL spectra are exciton luminescence from the GaN active layers in these two heterostructures. The peak position of the SCH GaN active layer was found to be ~10 meV higher than that of the DH GaN layer. The blue shift might be due to quantum confinement effects. By using the envelope function approximation approach,[13] the lowest confinement energy can be readily calculated, with electron the effective mass $m^* \sim 0.2m_0$ and the hole effective mass $m^* \sim 0.8m_0$,[14] to be ~10 meV for electrons and ~3 meV for holes in a 100-Å single GaN quantum well with $Al_{0.06}Ga_{0.94}N$ barriers. This estimation is consistent with the experimental observation. The strong and relatively broad emission structures at higher

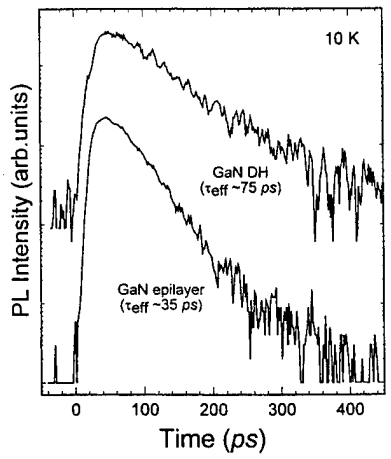

FIG. 4. Comparison of PL decay of exciton emissions in the GaN DH sample and an epilayer sample. The curves are vertically displaced for clarity.

energies are luminescence associated with AlGaN layers as labeled in the figure. The doublet spectral feature related to AlGaN alloys in the DH sample presumably arises from a small alloy concentration difference between two AlGaN cladding layers. If this is the case, the observed energy separation of ~25 meV suggests that slightly less than a 1% alloy concentration fluctuation occurred during the preparation of DH structure by MOCVD growth. However, the rather complicated spectral structure on the lower energy side of the main emission peak exhibited by the alloy waveguiding layers in the SCH sample cannot be simply assigned to the deviation in Al compositions between the two layers. This is an issue requiring further study.

We have also performed time-resolved PL measurements to study the dynamics of exciton luminescence in the GaN active layer of the DH structure. In order to avoid generating carriers in the AlGaN cladding layers and to prevent the profound effects of carrier diffusion from barrier layers into the active layer, the photon energy of the picosecond pulsed laser was tuned to very closely to the band gap of GaN with an excitation wavelength at ~345 nm. Figure 4 presents the time evolution of bound-exciton emission observed in the GaN/AlGaN DH sample, where a typical PL time-decay curve from a GaN epitaxial film taken under the same experimental conditions is also given for comparison. Both samples were deposited on SiC substrates under similar growth conditions except that the DH structure was deposited on top of one of them. As shown in the figure, the measured decay time for the bound exciton emission in the DH sample was found to be (~75 ps) twice as longer as that in the GaN epilayer (~35 ps). Recent exciton dynamic studies have revealed that the capture of excitons and trapping of carriers by nonradiative centers at defects and impurities play a major role in the recombination processes responsible for the exciton population decay in GaN samples.[15] However, it is unclear whether or not dislocations behave like nonradiative recombination centers. The results presented here suggest that dislocations most likely involve the nonradiative recombination processes. The increase in the exciton PL decay time observed in the DH sample indicates that the density of nonradiative recombination centers in the GaN active layer of the DH sample is smaller than that of the bare GaN epilayer. The AlGaN cladding layers could be a factor in the enhancement of the radiative recombination rate by reducing the density of dislocations in the GaN active layer, since it is known that a heterostructure system with built-in strain can significantly reduce the density of defects such as dislocations.[16] In addition, the deposition of a cladding layer on top of the GaN active layer could have passivated the surface states resulting in a reduction in the nonradiative recombination velocity of the photoexcited carriers on the bare surface and in its vicinity.

In conclusion, strong, sharp spectral structures associated with exciton transitions in GaN epitaxial layers and GaN/AlGaN heterostructures grown on 6H–SiC substrates by MOCVD were observed in photoluminescence and reflectance spectra. The observation of exciton transitions with lower energies in the epitaxial GaN based materials grown on SiC compared to that on sapphire substrates suggests that the GaN based epilayers on SiC substrates are subject to tensile strain, while those on sapphire substrates are under compression. The residual strain induced by lattice-parameter and thermal-expansion mismatch plays an important role in determining the exciton transition energies. In addition, our picosecond relaxation study of exciton decay dynamics suggests that for the GaN/AlGaN heterostructure samples, an AlGaN cladding layer with a small mole fraction AlN can be relatively effective in enhancing the radiative recombination rate for excitons as a result of reducing the density of dislocations and suppressing surface recombination velocity in the GaN active layer.

This work at OSU was supported by AFOSR, DARPA, ONR, and ARO. The work at CREE was supported by DARPA under Contract No. MDA972-95-C-0016. The work at NCSU was supported by ONR under Contract No. N00014-92-J-1477.

[1] J. I. Pankove, Mater. Res. Soc. Symp. Proc. **162**, 515 (1990), and references therein.
[2] S. Strite and H. Morkoç, J. Vac. Sci. Technol. B **10**, 1237 (1992), and references therein.
[3] H. Morkoç, S. Strite, G. B Gao, M. E. Lin, B. Sverdlov, and M. Burns, J. Appl. Phys. **76**, 1363 (1994).
[4] X. H. Yang, T. Schmidt, W. Shan, J. J. Song, and B. Goldenberg, Appl. Phys. Lett. **66**, 1 (1995).
[5] A. S. Zubrilov, V. I. Nikovlaev, V. A. Dmitriev, K. G. Irvine, J. A. Edmond, and C. H. Carter, Jr., Inst. Phys. Conf. Ser. **141**, 525 (1995).
[6] S. Nakamura, M. Senoh, S. Nagahama, N. Iwasa, T. Yamada, T. Matsushita, H. Kiyoku, and Y. Sugimoto, Jpn. J. Appl. Phys. **35**, L74 (1996).
[7] S. Nakamura, M. Senoh, S. Nagahama, N. Iwasa, T. Yamada, T. Matsushita, H. Kiyoku, and Y. Sugimoto, Appl. Phys. Lett. **68**, 2105 (1996).
[8] R. Dingle and M. Ilegeme, Solid State Commun. **9**, 175 (1971).
[9] B. Monemar, Phys. Rev. B **10**, 676 (1974).
[10] W. Shan, T. J. Schmidt, X. H. Yang, S. J. Hwang, J. J. Song, and B. Goldenberg, Appl. Phys. Lett. **66**, 985 (1995).
[11] B. Gil, O. Briot, and R.-L. Aulombard, Phys. Rev. B **52**, R17028 (1995).
[12] W. Rieger, T. Metzger, H. Angerer, R. Dimitrov, O. Ambacher, and M. Stutzmann, Appl. Phys. Lett. **68**, 970 (1996).
[13] G. Bastard, Phys. Rev. B **25**, 7584 (1982).
[14] *Landolt-Bornstein*, edited by O. Madelung, New Series, Group 3, Vol. 17a (Springer, Berlin, 1982).
[15] W. Shan, X. C. Xie, J. J. Song, and B. Goldenberg, Appl. Phys. Lett. **67**, 2512 (1995).
[16] Z. Liliental-Weber, H. Sohn, and J. Washburn, in *Semiconductors and Semimetals*, edited by E. R. Weber (Academic, Boston, 1993), Vol. 38, Chap. 9.

Optical transitions in $In_xGa_{1-x}N$ alloys grown by metalorganic chemical vapor deposition

W. Shan,[a] B. D. Little, and J. J. Song
Center for Laser Research and Department of Physics, Oklahoma State University, Stillwater, Oklahoma 74078

Z. C. Feng, M. Schurman, and R. A. Stall
EMCORE Corporation, Somerest, New Jersey 08873

(Received 22 July 1996; accepted for publication 20 September 1996)

We present the results of optical studies of $In_xGa_{1-x}N$ alloys ($0<x<0.2$) grown by metalorganic chemical vapor deposition on top of thick GaN epitaxial layers with sapphire as substrates. Photoluminescence (PL) and photoreflectance measurements were performed at various temperatures to determine the band gap and its variation as a function of temperature for samples with different indium concentrations. Carrier recombination dynamics in the alloy samples were studied using time-resolved luminescence spectroscopy. While the measured decay time for the alloy near-band-edge PL emissions was observed to be generally around a few hundred picoseconds at 10 K, it was found that the decay time decreased rapidly as the sample temperatures increased. This indicates a strong influence of temperature on the processes of trapping and recombination of excited carriers at impurities and defects in the InGaN alloys. © *1996 American Institute of Physics.* [S0003-6951(96)04748-1]

The quest for light emitting devices operating in blue and ultraviolet (UV) spectral regions has led to extensive studies on the properties of wide band-gap semiconductor materials for years. GaN based wide band-gap III–V nitride systems have recently attracted much attention as the most promising material for such device applications.[1–3] Among these, the $In_xGa_{1-x}N$ alloy system is of particular importance because its direct band gap covers a wide spectral range from UV (~365 nm for GaN band gap) to red (~650 nm for InN band gap).[4,5] In fact, recently commercialized superbright high-efficiency blue light emitting diodes and demonstrated current-injection laser diodes are all based on $GaN/In_xGa_{1-x}N$ heterostructures using $In_xGa_{1-x}N$ layers as the active light emitting medium.[6,7] In this report, we present the results of a study of the optical properties of $In_xGa_{1-x}N$ alloys ($0<x<0.2$) grown on top of thick GaN epilayers by metalorganic chemical vapor deposition (MOCVD). Photoluminescence (PL) measurements were performed to assess the optical properties of samples with different alloy compositions. Photomodulation spectroscopy was used to determine the energy gap of the samples and to examine the effect of temperature on the band gap. Transient luminescence measurements were carried out to study photoluminescence decay processes in the alloy samples.

The InGaN alloy samples used in this work were nominally undoped single-crystal epifilms grown by MOCVD. Before the depositions of alloys, thick GaN layers were grown on sapphire substrates at a temperature of ~1050 °C with 20-nm GaN buffers. The alloy layers were deposited at a temperature around 800 °C. The thicknesses of the $In_xGa_{1-x}N$ epitaxial layers were typically around a few thousand ångstroms. Optical measurements were carried out on the InGaN samples over a temperature range from 10 K up to room temperature (295 K). Samples were mounted onto the cold finger of a closed cycle refrigerator and cooled down to desired temperatures for the measurements. Photoluminescence spectra were measured using an experimental setup consisting of a HeCd laser as the excitation source and a 1-M double-grating monochromator connected to a photon-counting system. For photomodulation reflectivity measurements, quasimonochromatic light dispersed by a 1/2-M monochromator from a xenon lamp and a chopped HeCd laser modulating beam were focused on the samples and the reflected signals were detected by an UV-enhanced photomultiplier tube connected to a lock-in amplification and data acquisition system. For transient luminescence measurements, a frequency-doubled pulsed dye laser synchronously pumped by a frequency-doubled mode-locked Nd:YAG laser was used as the primary excitation source (2 ps, 76 MHz). The luminescence signals were dispersed by a 1/4 M monochromator and detected by a synchroscan streak camera with a temporal resolution of 2 ps. The overall time resolution of the system is less than 15 ps.

10-K photoluminescence (PL) and photoreflectance (PR) spectra of an $In_{0.14}Ga_{0.86}N$ sample are shown in Fig. 1. The PL spectrum (lower curve) exhibits two dominant spectral features: a sharp, strong emission line at higher energy arising from the near-band-edge excitonic transitions in GaN, and a relatively broad strong luminescence structure related to the alloy. The weak spectral structures observed between them were mainly luminescence signatures involving donor–acceptor-pair transitions in the GaN layer. The spectral feature with derivativelike line shapes on the lower-energy side of the PR spectrum (upper curve) corresponds to the optical transition associated with the alloy band gap, and the differential spectral structures at high energy are free-exciton transitions from the edges of different valence bands to that of the conduction band of wurtzite GaN. Photoreflectance is a spectroscopic method utilizing modulation of the built-in

[a]Electronic mail: wshan@osuunx.ucc.okstate.edu

 0003-6951/96/69(22)/3315/3/$10.00

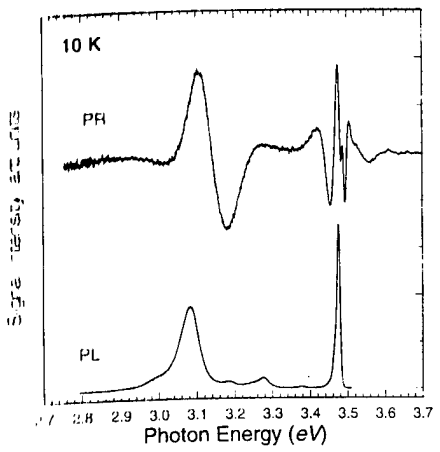

FIG. 1. PR (upper curve) and PR (lower curve) spectra of a $In_{0.14}Ga_{0.86}N$ sample at 10 K are shown for comparison.

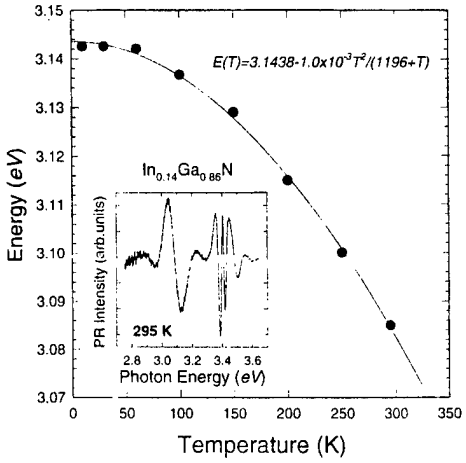

FIG. 2. Temperature dependence of interband transitions energy of the $In_{0.14}Ga_{0.86}N$ sample. The solid curve represents least-squares fits to the experimental data using Varshni empirical equation. The inset shows a room-temperature PR curve of the sample.

electric field in the samples. While a PR spectrum exhibits sharp derivativelike structures on a featureless background due to the optical modulation, the nature of the derivative is not immediately clear. Therefore, it is necessary to fit the PR curve to different line-shape functional forms[8,9] in order to determine the energy positions associated with the optical transitions. We found that using a third derivative Gaussian line-shape functional form which is appropriate for describing band-to-band transitions[10,11] results in a much better fit to the line positions and widths of the PR spectra than using a Lorentzian functional form.[12,13] This suggests that the optical transition observed at even the lowest temperature is of the nature of band-to-band transition rather than excitonic transition, presumably because of the strong inhomogeneous broadening due to alloying effects. The best fits to the 10-K PR spectral features yield an energy of 3.143 eV for the transition in $In_{0.14}Ga_{0.86}N$, indicating a large Stokes shift ($\sim$60 meV) between the PL peak position and the actual band-to-band transition energy.

With increasing temperature, the PL signal from the alloy layer quickly lost its intensity and spectral signature due to the increasingly enhanced nonradiative recombination processes and thermal broadening of the emission structures, whereas PR spectral structures associated with the InGaN band gap could be well resolved up to room temperature for all alloy samples used. Figure 2 shows the shift of optical transition energy as a function of temperature for the $In_{0.14}Ga_{0.86}N$ sample. The solid line in the figure represents the best fit to the Varshni empirical equation[14]

$$E_0(T) = E_0(0) - \alpha T^2/(\beta + T), \tag{1}$$

where $E_0(0)$ is the transition energy at 0 K, and α and β are constants referred to as Varshni thermal coefficients. The parameters obtained from the best fit for the sample are given in the figure. The better spectral resolution of PR spectroscopy compared to PL measurement enables us to determine the actual energy gaps for the InGaN alloy samples used in this work. In Fig. 3, we plot the measured energy gaps of various samples at 10 and 295 K against their alloy compositions, with 10-K PL results for comparison. Within the alloy composition range studied in this work, the PR results are in reasonably good agreement with the theoretical prediction for the dependence of the $In_xGa_{1-x}N$ band gap on In concentration including the bowing effect: $E(x) = 3.5 - 2.63x + 1.02x^2$ eV.[15] These measured values suggest that the uncertainty in determination of the alloy concentrations by x-ray measurements is $\sim$1%. On the other hand, the scattered PL data, as indicated by the figure, are apparently not a reliable way to map energy gap evolution for the alloy system because the PL signals are most likely associated with impurities and the effects of alloy disorder broadening.

We have also performed time-resolved PL measurements to study carrier recombination dynamics in the $In_xGa_{1-x}N$ samples. Figure 4 shows the temporal evolution of spectrally integrated luminescence associated with an $In_{0.08}Ga_{0.92}N$ sample as selected temperatures. The time evolution of the luminescence is dominated by exponential decay with a measured effective lifetime around 340 ps at 10 K. The temporal profile of the luminescence gradually evolved into an increasingly nonexponential decay with a drastic decrease of the effective lifetime for the main decay

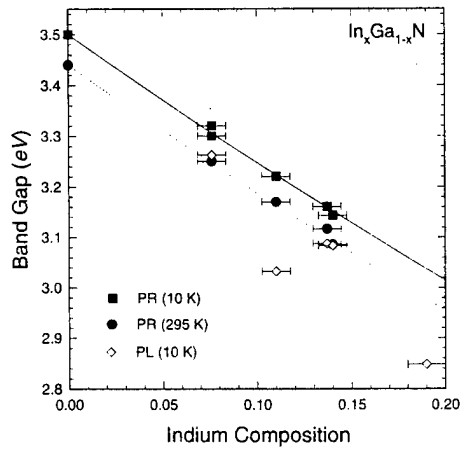

FIG. 3. Energy gaps of various samples measured by PR at 10 K and 295 K vs their alloy compositions. 10-K PL results are shown for comparison. The solid line is the theoretical prediction for the dependence of the $In_xGa_{1-x}N$ band gap on In concentration. The dotted line is that for room temperature (295 K) data.

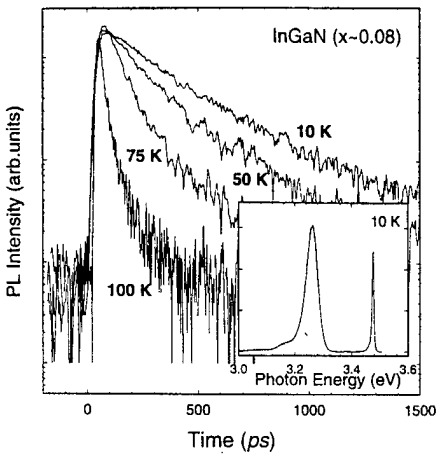

FIG. 4. Temporal variation of the alloy PL peak for an $In_{0.08}Ga_{0.92}N$ sample at selected temperatures. The inset shows the 10-K PL spectrum over a broad spectral range.

process as the sample temperature increased. At temperatures around 150 K, the deduced lifetime for the PL decay has already reached the limit of our instrumental resolution of 15 ps. Similar results were obtained for all samples used in this work: the measured decay time for near-band-edge PL emissions was generally around a few hundred picoseconds at 10 K, and it decreased rapidly as sample temperatures increased. The measured decay time was examined as a function of energy positions of the 10-K PL peak shown in the inset of Fig. 4. The reason for doing so is to verify whether the PL structure resulted from recombination of localized excitons or emission directly involving impurity states and alloy potential fluctuations.[16,17] If the PL emission originated from localized excitons in the InGaN alloys, the lifetime is predicted to follow the so-called power-law dependence,[18] i.e., $\tau \propto E_{BX}^{3/2}$, where E_{BX} is the exciton localization energy. That means the measured lifetimes increase with increasing exciton localization energy which corresponds to a decrease in electron-hole wave function overlap. Our experimental results did not exhibit such a three-halves dependence of measured effective lifetime upon the energy position, suggesting impurity states and alloy potential fluctuations are most likely responsible for the alloy PL signals.

Although the radiative recombination processes involved in PL emissions in the InGaN samples are not of excitonic nature as mentioned previously it is still worthy to make a comparison of the results obtained in this work with the excitonic emission decay processes observed in pure GaN.[19] While the measured effective lifetime for PL decay in InGaN samples was found to be an order of magnitude longer than that in GaN, the dependence of the PL decay process on the temperature in InGaN alloys is much stronger than that in GaN.[20] Such a strong temperature influence suggests that although recombination from carriers bound to extrinsic states such as defects or impurities can be very efficient at low temperatures, the measured decay time is still determined by detailed decay kinetics in the alloy samples. The observed decrease of the PL decay time along with the increasingly nonexponential transient characteristics with temperature indicates that incrementally stronger nonradiative relaxations occur as the temperature increases, resulting in continued faster decay of the photogenerated carrier population. The decrease of PL in both intensity and observed effective lifetime with temperature suggests that nonradiative processes including trapping and recombination at energy levels associated with impurities and defect centers at or near the midgap (Shockley–Read–Hall recombination), surface recombination, and Auger recombination prevail in the InGaN alloys at relatively high temperatures. It is well known that the lifetime of photogenerated carriers is strongly dependence on the sample quality for semiconductor alloy systems.[17] The observations reported here indicate that the impurities and defects incorporated during the InGaN epitaxial growth generate PL quenching centers in the layers which adversely affect the carrier radiative recombination.

In conclusion, we have studied optical transition processes in $In_xGa_{1-x}N$ alloys using a few different approaches including both conventional and time-resolved PL measurements as well as PR spectroscopy . The highly sensitive PR spectroscopy allows us to unambiguously determine the band gap energy for the alloy samples within the alloy composition range ($0<x<0.2$) studied. We found that the low-temperature PL emission from alloy layers are primarily recombinations directly involving impurity states and alloy potential fluctuations. Strong dependence of PL decay on temperature observed in the various alloy samples indicates that the trapping and recombination of photogenerated carriers at impurities and defect centers are dominant channels in determining the carrier population decay process.

This work at OSU was supported by AFOSR, ARO, DARPA, and ONR.

[1] S. Strite and H. Morkoç, J. Vac. Sci. Technol. B **10**, 1237 (1992), and references therein.
[2] J. I. Pankove, Mater. Res. Soc. Symp. Proc. **162**, 515 (1990), and references therein.
[3] H. Morkoç, S. Strite, G. B. Gao, M. E. Lin, B. Sverdlov, and M. Burns, J. Appl. Phys. **76**, 1363 (1994).
[4] K. Osamura, S. Naka, and Y. Murakami, J. Appl. Phys. **46**, 3432 (1975).
[5] See, for example, S. Nakamura, T. Mukai, and M. Senoh, J. Appl. Phys. **76**, 8189 (1994).
[6] S. Nakamura, M. Senoh, S. Nagahama, N. Iwasa, T. Yamada, T. Matsushita, H. Kiyoku, and Y. Sugimoto, Jpn. J. Appl. Phys. 1 **35**, L74 (1996).
[7] S. Nakamura, M. Senoh, S. Nagahama, N. Iwasa, Y. Yamada, T. Matsushita, H. Kiyoku, and Y. Sugimoto, Appl. Phys. Lett. **68**, 2105 (1996).
[8] D. E. Aspnes, in *Optical Properties of Solids*, edited by M. Balkanski (North-Holland, Amsterdam, 1980), Chap. 4A.
[9] F. H. Pollak and O. J. Glembocki, Proc. SPIE **946**, 2 (1988).
[10] O. J. Glembocki and B. V. Shanabrook, Superlattices Microstruct. **5**, 235 (1987).
[11] H. Shen, S. H. Pan, F. H. Pollak, M. Dutta, and T. R. AuCoin, Phys. Rev. B **36**, 9384 (1987).
[12] O. J. Glembocki and B. V. Shanabrook, in *Semiconductors and Semimetals*, edited by D. G. Seiler and C. L. Little (Academic, New York, 1992), Vol. 36, Chap. 4.
[13] F. H. Pollak and H. Shen, Mater. Sci. Eng. R **10**, 275 (1993).
[14] Y. P. Varshni, Physica **34**, 149 (1967).
[15] A. F. Wright and J. S. Nelson, Appl. Phys. Lett. **66**, 3051 (1995).
[16] M. Voos, R. F. Leheny, and J. Shah, in *Optical Properties of Solids*, edited by M. Balkanski (North-Holland, Amsterdam, 1980), Chap. 6.
[17] L. Pavesi and M. Guzzi, J. Appl. Phys. **75**, 4779 (1994).
[18] E. I. Rashba and G. E. Gurgenishvili, Sov. Phys. Solid State **4**, 759 (1962).
[19] W. Shan, X. E. Xie, J. J. Song, and B. Goldenberg, Appl. Phys. Lett. **67**, 2512 (1995).
[20] J. J. Song, W. Shan, T. Schmidt, X. H. Yang, A. Fischer, S. J. Hwang, B. Taheri, B. Goldenberg, R. Horning, A. Salvador, W. Kim, Ö. Aktas, A. Botchkarev, and H. Morkoç, Proc. SPIE 86 (1996).

Inst. Phys. Conf. Ser. No 145: Chapter 9
Paper presented at 22nd Int. Symp. Compound Semiconductors, Cheju Island, Korea, 28 August–2 September 1995

Recent Progress in Optical Studies of Wurtzite GaN Grown by Metalorganic Chemical Vapor Deposition

W. Shan, T. Schmidt, X.H. Yang, and J.J. Song

Center for Laser Research and Department of Physics, Oklahoma State University, Stillwater, Oklahoma 74078, USA

B. Goldenberg

Honeywell Technology Center, Plymouth,, Minnesota 55441, USA

Abstract. We present the recent results of our spectroscopic studies on optical properties of GaN grown by metalorganic chemical vapor deposition, including the issues vital to device applications such as stimulated emission and laser action, as well as carrier relaxation dynamics. By optical pumping, stimulated emission and lasing were investigated over a wide temperature range up to 420 K. Using a picosecond streak camera, free and bound exciton emission decay times were measured. In addition, the effects of pressure on the optical interband transitions and the transitions associated with impurity/defect states were studied using diamond-anvil pressure-cell technique.

1. Introduction

GaN based wide band-gap III-V nitride semiconductors currently attract extensive attention for their potential electronic and optoelectronic device applications such as UV-blue LED's and laser diodes.[*1-3*] Recent demonstration of superbright high-efficient blue LED's based on nitride heterostructures by the Nichia group and others[*4*] and the reports on observation of optically pumped stimulated emission in GaN epifilms by a few groups[*5,6*] have led to much more intense interest in the development of efficient nitride UV-visible light emitters. In this report, we present recent results of our spectroscopic studies on the optical properties of GaN grown by metalorganic chemical vapor deposition (MOCVD).

2. Experimental details

The GaN samples used in this study were all nominally undoped single-crystal films grown on (0001) sapphire substrates by MOCVD. Various optical measurements were carried out on the GaN samples over a temperature range typically from 10 K to room temperature (295 K). Conventional photoluminescence (PL) spectra were measured with a cw HeCd laser (325 nm) as an excitation source and a 1-M double-grating monochromator connected to a photon-counting system. Time-resolved photoluminescence (TRPL) measurements were performed using a frequency tunable pulsed laser (2 ps pulse duration, 82MHz) as an excitation source and

a streak camera (2 ps resolution), in conjunction with a 1/4-M monochromator as a detection system. Pressure-dependent PL measurements were conducted using the diamond-anvil pressure-cell technique. Stimulated emission and lasing experiments were carried out employing side-pumping geometry using a nanosecond pulsed laser (10 Hz) as the optical pumping source.

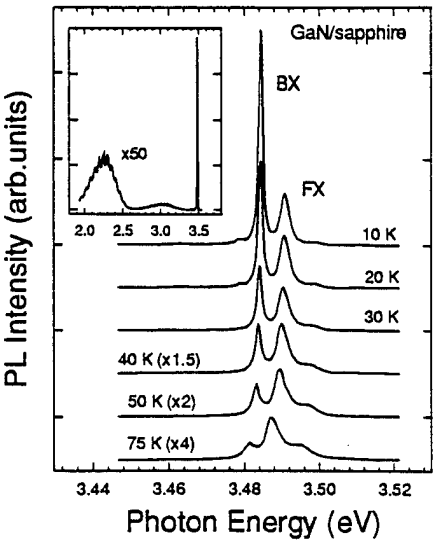

Fig. 1. Exciton luminescence spectra of a MOCVD GaN sample taken at different temperatures. The inset shows the 10 K PL spectrum of the sample over a broad spectral range.

3. Results and discussions

To illustrate the quality and purity of the GaN epifilm samples used in this work, PL spectra taken from the samples are shown in Fig. 1. All GaN samples exhibit strong, predominant near band-edge exciton luminescence lines corresponding to the radiative decay of excitons at low temperatures. The inset shows a broad range of the typical PL spectrum taken at 10 K. The broadband yellow emission and a weak emission band in the blue spectral region could be observed. The strongest emission line marked by BX in Fig. 1 has a full width at half maximum (FWHM) of less than 1.0 meV at 10 K. The second one labeled FX in the figure shows a FWHM of less than 1.5 meV, indicating the high quality, as well as substantial purity of the samples. The intensity of the BX peak was found to decrease much faster than that of the FX as the temperature increased. It became hardly resolvable when the temperature was raised to above 100 K (not shown). Such variations of the luminescence intensity as a function of temperature indicate that the emission line can be attributed to the radiative recombination of excitons bound to neutral donors. The second strongest luminescence line, together with the weak emission feature on the higher energy side, can be assigned to intrinsic free-exciton emissions.

3.1 Optically pumped stimulated emission and lasing

Strong stimulated emission and lasing at near-UV wavelengths could be observed from the GaN samples over a broad temperature range from 10 K to ~ 420 K by optical pumping with a tunable nanosecond laser. In Fig.2 we plot the emission spectra taken at 375 K for pumping power densities below and above the estimated threshold. Under low-excitation conditions, the spectrum is characterized by a very broad spontaneous emission band with the maximum position at 376 nm. With increasing pumping power densities, a new feature with a narrower linewidth appears on the low energy side of the spontaneous emission band and becomes predominant as the pumping power densities are further increased. The emission feature is found to exhibit superlinear increase in intensity and a red shift in the peak position as the pumping power increases. In addition, the longitudinal cavity modes of lasing in some samples

with small cavity lengths could be clearly observed with a CCD camera. An example is given in the inset of Fig.2, where the resonant cavity length of the sample is about 200 μm thick. The resonant cavity of the samples was prepared just by cutting the large wafer into bar-like specimens with a diamond saw. The resulting sample edges are far from mirror-like facets.

The threshold pumping power was estimated to be ~500 kW/cm^2 at 10 K and ~800 kW/cm^2 at room temperature. Generally, the lasing threshold varies from sample to sample. For a given optical pumping source, the most important influence on the threshold is from the sample itself. This can be classified into two groups: one is associated with material properties, such as impurities, crystallinity, and defects; the other is related to the sample preparation such as the laser cavity length and the quality of sample edge facets. We expect that the lasing threshold in GaN can be lowered substantially by better preparing the sample edge facets, for example, with reflective coating. With better designed laser structures, such as double-heterostructures, the lasing threshold is also expected to be significantly lowered. Recently, Zubrilov *et al.* reported the observation of multipass stimulated emission with Fabry-Perot modes from GaN grown on 6H-SiC substrates.[6] In this case, the interference fringes originated from the microcavities. These cavities were formed by microcracks, which were generated during the cleaving process. As better lattice-matched substrates become available for epitaxial growth of GaN with better crsytallinity, the lasing threshold is expected to be lowered further.

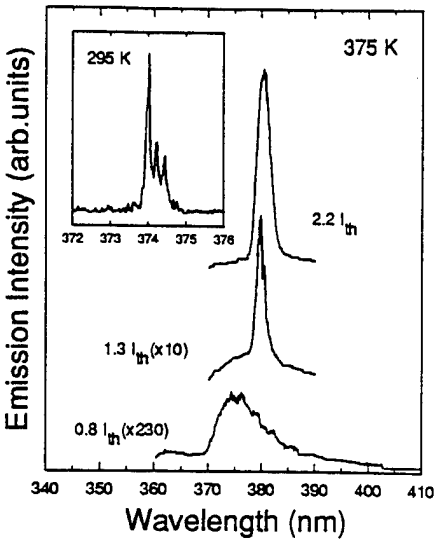

Fig. 2. Emission spectra of GaN at 375 K under different pumping power densities. The inset shows the emission spectrum taken at room temperature (295 K) exhibiting longitudinal mode fringes.

We also noted that the threshold is not very sensitive to the change of sample temperature. It is known that high-temperature sensitivity of the lasing threshold usually limits the performance of a laser in high temperature operations.[7] The weak temperature dependence of the lasing threshold suggests that laser operations can be substantially extended to the high temperature range. Thus the results reported here imply that GaN based laser diodes have the potential of operating with a much higher temperature tolerance compared to conventional semiconductor laser diodes.

3.2 Radiative decay of free excitons and bound excitons

The temporal evolution of spectrally integrated exciton luminescence for both free-exciton (FX) and bound-exciton (FX) emissions observed in a GaN sample at 10 K is shown in Fig. 3. The overall time resolution of the experimental system used for conducting the measurements is less than 15 ps. The time evolution for both FX and BX luminescence is dominated by exponential decay. The lifetime of the main PL decay was found to be ~35 ps for the FX emissions and ~55 ps for the BX emissions for the GaN sample at 10 K. It should be pointed out that the

measurement of luminescence decay time does not provide a direct measurement of radiative lifetime and that the measured PL decay time yields only an effective lifetime (τ_{eff}) for free excitons and bound excitons. It involves both the radiative (τ_R) and nonradiative (τ_{NR}) lifetimes with the decay rate expressed as

$$1/\tau_{eff}=1/\tau_R+1/\tau_{NR}. \qquad (1)$$

The radiative lifetime for an excited state in a semiconductor can be estimated by considerations of optical transition probability. The radiative lifetime τ_R of the excited state can be described by:[*8,9*]

$$\tau_R=2\pi\epsilon_0 m_0 c^3/\tilde{n}e^2\omega^2 f, \qquad (2)$$

where f is the oscillator strength of the optical transition, $\tilde{n}$ is the refractive index, and the other symbols have their usual meanings. By using $\tilde{n}$=2.4, and ω=~5.3x10^{15}sec^{-1} for GaN, one can roughly obtain τ_R~(800/f) ps. The radiative lifetime of bound excitons in GaN is expected to be just slightly shorter than one nanosecond if we take the upper limit with its oscillator strength as unity (f~1). The oscillator strength of free excitons calculated within the effective-mass approximation is given by $f=E_p/\pi\hbar\omega(V/a_x^3)$, where E_p is the Kane matrix element connecting Bloch states in the valence and conduction bands, V is the volume of unit cell, and a_x is the effective Bohr radius of free exciton. Our result yields f~*0.012* for the free excitons in GaN using E_p~18 eV and a_x~20 Å. Thus, the calculated value of the radiative lifetime for free excitons in GaN will be in several tens of nanoseconds domain. The discrepancy between the measured values of PL decay time and the theoretical estimated radiative lifetime can be attributed to nonradiative relaxation processes in competition with the radiative channel. In the case where nonradiative decay rate is larger, the measured decay time is characteristic for the nonradiative processes in accordance with Eq.(1). This situation is typical for recombination from intrinsic states of semiconductors. The nonradiative processes such as multiphonon emission captured by deep centers, Auger effect, etc., give rise to fast relaxation of the excited carriers down to lower states from which they decay radiatively or relax nonradiatively. As a result, the measured PL decay time for a given excited state is an effective lifetime and usually much shorter than a radiative one. This has been observed in a number of semiconductor bulk materials and heterostructures with the measured free-exciton PL decay time decreasing progressively as the density of nonradiative recombination centers increased.[*9*] The slow rise of bound-exciton luminescence intensity compared to that of the free-exciton PL shown in Fig. 3 is one indicator of such nonradiative relaxation processes for the free excitons relaxing to the bound excitons. We found that the capture of excitons and trapping of carriers by such nonradiative centers as defects and impurities play a major role in the recombination processes responsible for the exciton population decay in the GaN samples studied in this work. The measured PL decay time was found to be directly related to the intensity of broadband emissions lying in the GaN band gap. The broad emission structure referred to as yellow emission in the literature is believed to be associated with the optical

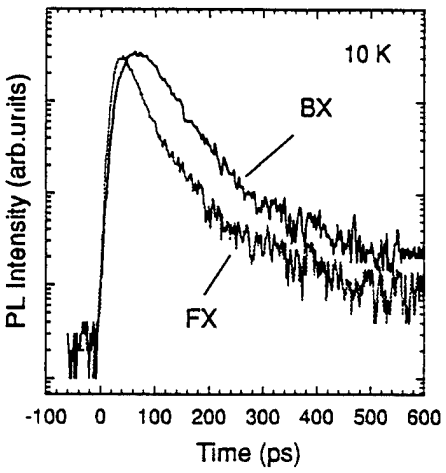

Fig. 3. Temporal variation of spectrally integrated PL for both intrinsic free-exciton and bound-exciton emissions.

transitions between the energy levels involving impurity and/or defect states. The intensity of yellow emission is likely to be proportional to the density of defects and impurities present in samples. We found that the stronger the yellow emission, the shorter the PL decay time in a GaN sample. Fig. 4 shows a comparison of free-exciton PL decays taken from two samples under identical excitation conditions. The yellow emission intensities of the two samples are drastically different, with approximately a 100:1 ratio. The lifetime of free-exciton emission in the sample with stronger yellow emission was deduced to only 15 ps (which is the limit of our instrumental resolution). Therefore, the fast decay behavior of the PL intensity in this sample indicates that the capture of excitons and trapping of carriers at defects and impurities through nonradiative combinations appear to dominate the decay of exciton population. The process of capture is dependent on the density of defects and impurities in the GaN samples.

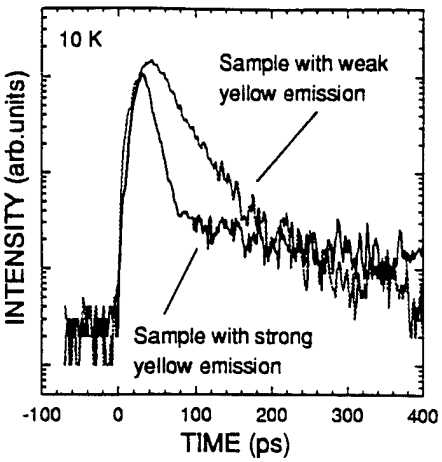

Fig. 4. Comparison of the decay times of free-exciton emission between two GaN samples with the relative intensity ratio of 100:1 for the yellow emission.

3.3 Pressure coefficient and hydrostatic deformation potential for direct Γ band gap

In Fig. 5 we plot the peak energies of exciton emission and yellow emission structures as a function of pressure. The solid lines in the figure are the least-square fits to the experimental data using the quadratic-fit function

$$E(P)=E(0)+\alpha P+\beta P^2. \qquad (3)$$

The change of the intense and sharp BX transition with pressure plotted in the figure provides an unmistakable signature of the direct Γ band-gap dependence for wurtzite GaN based on the effective mass approximation. The best fits to the data yield a linear slope of 3.86×10^{-3} eV/kbar with an extremely small sublinear term of -8×10^{-7} eV/kbar^2. Similar results can be obtained from fitting the FX transition as well ($\alpha=3.9\times10^{-3}$ eV/kbar and $\beta=-1.8\times10^{-6}$ eV/kbar^2).

The application of hydrostatic pressure allows a direct estimation of the hydrostatic deformation potential for the direct Γ band gap of wurtzite GaN. The deformation potential is defined as $a=\partial E/\partial \ln V$. The hydrostatic deformation potential for the direct Γ band gap of wurtzite GaN could be deduced as $a=-9.2\pm1.2$ eV.

The broad yellow emission band maximum was found to shift with pressure at a rate of 4.0×10^{-3} eV/kbar, almost the same as that of exciton emissions. This spectral structure could be commonly observed in the PL spectra of nominally undoped GaN single crystals regardless of the crystal growth techniques. More strikingly, this band was observed in samples implanted with a variety of atomic species.[*10*] These results have led to the general belief that the broadband emission in the yellow spectral region involves defects. Recent theoretical studies on the electronic structures of impurities and native defects in GaN have suggested that point

defects, such as antisites and vacancies, play important roles.[*11-14*] The pressure dependence of the yellow emission band, in broad terms, is consistent with the transitions involving shallow donors and deep acceptors. Further theoretical and experimental studies are necessary to investigate the microscopic nature of the broadband yellow emission in GaN.

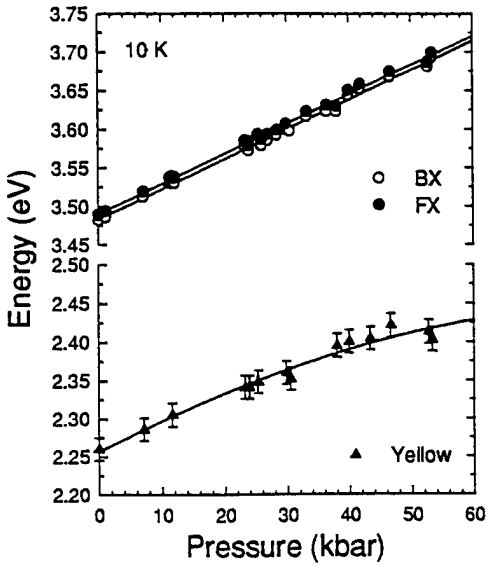

Fig. 5. Dependence of the energy positions on pressure for the various observed PL transitions in the GaN sample.

4. Conclusions

Optically pumped stimulated emission and lasing phenomena in GaN on sapphire were investigated using high-power pulsed lasers. Stimulated near-violet emissions were observed over a wide temperature range from 10 K to ~420 K. The dynamics of photoexcited excess carriers in high quality GaN samples were investigated. This was done using transient luminescence spectroscopy in the picosecond regime using a streak camera in the region of near band-edge excitonic emissions. We found that the strong capture of photo-excited carriers in impurities and/or defects through nonradiative recombination processes dominates the decay of carrier population. The capture process depends on the density of impurities and defects in the GaN samples. The effects of pressure on the various optical transitions associated with both intrinsic and extrinsic processes in the GaN samples were examined by photoluminescence spectroscopy. The pressure coefficient of the GaN band gap was determined by studying the shift of exciton emission lines in GaN with applied pressure. Our results yielded the variation of the GaN band gap with pressure to be $\Delta E(P)=3.9\times10^{-3}P-1.0\times10^{-6}P^2$ eV. The deformation potential for the direct Γ band was also deduced from the experimental results to be -9.2±1.2 eV.

References

[*1*] Strite, S. and H. Morkoç, 1992, J. Vac. Sci. Technol. **B10**, 1237, and references therein.
[*2*] Pankove, J.I. 1990, Mater. Res. Soc. Symp. Proc. **162**, 515, and references therein.
[*3*] Morkoç, H. *et al.* 1994, J. Appl. Phys. **76**, 1363, and references therein.
[*4*] See, for example, Nakamura, S. *et al.* 1994, Appl. Phys. Lett. **64**, 1687.
[*5*] Yang, X.H. *et al*, 1995, Appl. Phys. Lett. **66**, 1.
[*6*] Zubrilov, A.S. *et al.* 1995, Inst. Phys. Conf. Ser. No.141, 525.
[*7*] Agrawal, G.P. and N.K. Dutta, 1993, in *Semiconductor Lasers*, (Van Nostrand Reinhold, New York), p.132.
[*8*] Dexter, D.L. 1958, in *Solid State Physics*, ed. F. Seitz and D. Turnbull (Academic, New York), Vol.6.
[*9*] 't Hooft, G.W. *et al.* 1987, Phys. Rev. **B35**, 8281.
[*10*] Pankove, J.I. and J.A. Hutchby, 1976, J. Appl. Phys. **47**, 5387.
[*11*] Jenkins, D.W. and J.D. Dow, 1989, Phys. Rev. **B39**, 3317.
[*12*] Tansley, T.L. and R.J. Egan, 1992, Phys. Rev. **B45**, 10942; 1993, Physica **B 185**, 190.
[*13*] Neugebauer, J. and C.G. Van de Walle, 1994, Phys. Rev. **B50**, 8067.
[*14*] Boguslawski, P. *et al.* 1995, Phys. Rev. **B51**, 17255.

Submitted to PRB

Femtosecond Four-Wave-Mixing Studies of Nearly Homogeneously Broadened Excitons in GaN

A. J. Fischer, W. Shan, G. H. Park, and J. J. Song
Department of Physics and Center for Laser Research, Oklahoma State University, Stillwater, Oklahoma 74078.

D. S. Kim and D. S. Yee
Department of Physics, Seoul National University, Seoul 151-742, Korea

R. Horning and B. Goldenberg
Honeywell Technology Center, Plymouth, Minnesota 55441

Abstract

Femtosecond degenerate four-wave-mixing (FWM) is used to study coherent dynamics of excitons in GaN epilayers. Spectrally-resolved (SR) FWM data are dominated by the A and B intrinsic excitonic resonances. SR-FWM combined with time-integrated (TI) FWM demonstrates that the excitonic resonances are nearly homogeneously broadened even at low temperature. The temperature dependent dephasing rate is used to deduce exciton-phonon interaction rates. TI-FWM shows a strong beating between the A and B excitons and the beats are shown to be true quantum beats. In addition, a 180 degree phase shift in the quantum beating was observed when the polarization geometry was changed from co-linear to cross-linear.

Recently, there has been tremendous interest in GaN and related materials, due to its ability to emit light in the blue/UV region [1]. Many types of linear optical spectroscopy have been used to study these wide band gap semiconductors [2]. Nevertheless, significant uncertainties still remain regarding the fundamental band edge transitions in GaN. For instance, due to strong absorption in GaN and poor sample quality for thin layers (< 1μm), unambiguous determination of the exciton linewidth as a function of temperature by absorption is difficult, and as a result, exciton-phonon interaction rates are not well known. In addition, clear evidence of free excitons in the absorption spectra is still lacking.

Another area of intense research activity has been the coherent spectroscopy of semiconductors and their quantum wells, stimulated in part by the ready availability of tunable femtosecond laser sources. Extensive studies have been performed on GaAs, ZnSe, and related materials and their quantum wells in the coherent regime [3,4]. However, up to now, no studies have been performed on GaN in the femtosecond coherent regime.

In this paper, we present the results of the first femtosecond four-wave-mixing (FWM) studies on nearly homogeneously broadened excitons in a high quality GaN epilayer sample. We have performed time-integrated (TI) FWM and spectrally-resolved (SR) FWM as a function of temperature and polarization. From these studies, we have determined exciton-acoustic phonon and exciton-optical phonon coupling constants. TI-FWM displays well defined beating between the A and the B excitons, and SR-FWM demonstrates that the beating is due to true quantum beats between these two modes, and not due to the so called polarization beat [5]. In addition, the quantum beat between the A and the B excitons shows a 180 degree phase shift between the co-linear and the cross-linear polarization geometries. This is analogous to the heavy-hole (HH) and

light-hole (LH) exciton quantum beat in GaAs quantum wells, which also shows a 180 degree phase shift between the two polarization geometries [6].

We used the second harmonic of a self-mode-locked Ti:Sapphire laser in the high energy region of the tuning curve (700 nm). The second harmonic of the 100 fs pulses resonantly excites intrinsic excitons in the GaN epilayer. The 7.2 micron thick epilayer was grown with the wurtzite structure on a c-plane sapphire substrate using metalorganic chemical vapor deposition (MOCVD). The valence band degeneracy for wurtzite crystals is removed by crystal field splitting and spin-orbit interaction. As shown in the inset of fig. 2a, the two lowest energy transitions at the Γ point are the Γ^{V}_{9} - Γ^{C}_{7} exciton (A exciton transition) and the Γ^{V}_{7} (upper band) - Γ^{C}_{9} exciton (B exciton transition). FWM was performed on the A and B exciton transitions in the reflection geometry with an average power per beam of about 1 mW focused onto a 100 micron spot.

In Fig. 1a, TI-FWM data are shown at three different temperatures (T=10, 70, and 190 K). The laser was tuned near resonance with the B exciton, and the weak beating at 10 K is a result of the excitation of a small A exciton component. At 190 K, the FWM signal is nearly time-resolution limited. The decay time at each temperature was fit to single exponential decay to determine the decay rate as a function of temperature. The homogeneous linewidth can then be determined from the relation $\Gamma_{hom} = 2\hbar/T_2$, where T_2 is the pure dephasing time. In order to determine T_2 we need to know if the resonances are predominantly homogeneously or inhomogeneously broadened. This is because the FWM decay time τ_{FWM} is equal to $T_2/2$ in the homogeneously broadened limit and $T_2/4$ in the inhomogeneously broadened limit [7]. As discussed below, we have determined that the excitonic resonances studied here are nearly homogeneously broadened. Fig. 1b shows the homogeneous linewidth plotted as a function of temperature assuming homogeneous broadening.

Initially, the rate is linear with T, but begins to be superlinear starting from about 150 K. This indicates the dominance of the acoustic phonons as the scattering mechanisms for the dephasing of excitons at low temperature. At higher temperature, it is expected that optical phonons begin to contribute. We fit the decay rate $1/\tau_{FWM}$ to the following standard formula [8,9]:

$$\Gamma = \Gamma_o + \gamma T + \frac{\Gamma_{LO}}{\exp(E_{LO}/k_B T) - 1}$$

where Γ_o, γ, and Γ_{LO} are constants to be determined from the fit, and E_{LO} and k_B are, respectively, the optical phonon energy of GaN (91.7 meV) and Boltzmann's constant. The best fit is the solid line in Fig. 1b, achieved with the fitting parameters: $\Gamma_o = 2.4$ meV, $\gamma = 16$ μeV/K, and $\Gamma_{LO} = 390$ meV. These values are much larger than those for GaAs and GaAs quantum wells [9]. This is not so surprising, for GaN has larger effective masses for both electrons and holes in comparison with GaAs, and thus a much larger density of states. On the other hand, γ is comparable to that of ZnSe and ZnCdSe quantum wells, whereas Γ_{LO} is still much larger than that of ZnSe and related materials [4]. This is an interesting point, for the density of states of ZnSe as well as its polarity are comparable to those of GaN. The much larger Γ_{LO} for GaN should in part be due to the much larger E_{LO} of GaN in comparison to ZnSe (91 vs 30 meV). In addition, it is possible that larger deformation potential interaction, which may account for significant fraction of Γ_{LO} other than the Fröhlich interaction, is responsible for larger Γ_{LO}.

To determine whetherthe excitons are homogeneously or inhomogeneously broadened, we performed SR-FWM The advantage of SR-FWM is that it can give the exciton linewidths without any background, which plagues the analysis of absorption experiments. In addition, for high quality,

relatively thick epilayer samples, it is virtually impossible to perform absorption.

In Fig. 2, SR-FWM data at zero delay are plotted at several temperatures. Both the A and the B excitons are clearly present, and the SR-FWM data shown in Fig. 2 represent a very clear demonstration of the A and the B excitons without the interference of bound excitons that make the interpretation of photoluminescence spectra difficult. The SR-FWM linewidth at 10 K, the lowest temperature of our experiments, is about 2.5 meV for the B exciton, and about 2.1 meV for the A exciton. From TI-FWM and the fit shown in Fig. 1, the homogeneous linewidth in the low temperature limit is about 2.4 meV assuming homogeneous broadening, and 1.2 meV assuming inhomogeneous broadening. Therefore, even in the low temperature limit, the *minimum* homogeneous linewidth of our excitons is about half the total linewidth observed in SR-FWM. On the other hand, the observed linewidth is nearly equal to what is expected in the homogeneously broadened limit. At higher temperature, there is no doubt that the excitons we probe by FWM are predominantly homogeneously broadened. From these observations, we conclude that our excitons can be considered mostly homogeneously broadened even at the low temperature.

The relatively fast scattering at low temperature is most likely due to scatterings with *microscopic* impurities. On the other hand, since the total linewidth is roughly the sum of the homogeneous and the inhomogeneous broadenings [10], we can put the upper limit to the inhomogeneous broadening in our sample caused by the macroscopic variations in the sample quality. For both the A and the B excitons, it is less than 1.5 meV, and most likely in the range of a few tenths of an meV. Therefore, with further reduction of the defect density, achieving GaN exciton linewidths of less than 1 meV should be possible.

We now discuss the quantum beat between the A and the B excitons observed by TI and SR-FWM. As shown in Fig. 3, when we tune the laser roughly in the middle of the A and B exciton, well defined beating, whose period coincides with $(E_B-E_A)/h$, is observed (E_A , E_B = energy of the A and the B excitons observed in SR-FWM, respectively). However, the beating observed in TI-FWM in itself does not imply the existence of charge oscillation in the coherent superposition of A and B excitons. To prove that it is really a quantum beat, we probe the relative phase of the beating at different energies [5]. In Fig. 3, TI-FWM is plotted as a function of delay for several different energy positions across the B-exciton resonance. The phases are completely in synch at all the energies, which indicates that the beating we observe in TI-FWM is indeed due to the coherent superposition of the A and the B excitons.

Having established the quantum nature of the beating observed in TI-FWM, we now turn our attention to the polarization dependence of the quantum beat. In Fig. 4, TI-FWM in both the co-linear (solid lines) and the cross-linear (dotted lines) polarization geometries are shown. The maxima at one geometry correspond to the minima at the other, which indicates the existence of a 180 degree phase shift between the quantum beats. Similar observations have been made in case of the HH-LH quantum beat in GaAs quantum wells, and was theoretically described by including the total angular momentum for the conduction band (J=1/2) and valence band (J=3/2) in the optical Bloch equations [6]. In our case, the phase shift is likely to be caused by the different spin states of holes in the Γ_7 and the Γ_9 valence bands.

In conclusion, we have performed the first femtosecond coherent spectroscopy on excitons in a high quality GaN epilayer grown on a sapphire substrate. By the combined analysis of the TI-FWM and SR-FWM, we found that our excitons are nearly homogeneously broadened. We have

deduced the exciton-phonon interaction rates, and observed a beating in TI-FWM which we identified as a quantum beat between the A and the B excitons. Finally, we observed a clear 180 degree phase shift between the quantum beats in the collinear and the cross-linear polarization geometries, which we explain by differences between total angular momentum of the conduction band and the A and B valence bands.

We would like to thank Dr. L. J. Sham for helpful discussions. This work was supported by a joint grant of NSF and KOSEF(965-0200-003-2). The work at OSU was also supported by DARPA and ARO and the work at SNU was supported by the Ministry of Education (BSRI96-7401).

References

[1] S. Nakamura, M. Senoh, S. Nagahama, N. Iwasa, T. Yamada, T. Matsushita, H. Kiyoku, and Y. Sugimoto, Jpn. J. Appl. Phys. **35**, L74 (1996).

[2] W. Shan, T. Schmidt, X.H. Yang, J.J. Song, and B. Goldenberg, J. Appl. Phys. **79,** 3691 (1996); G.D. Chen, M. Smith, J.Y Lin, H.X. Jiang, A. Salvador, B.N. Sverdlov, A. Botchkarev, and H. Morkoç, J. Appl. Phys. **79,** 2675 (1996).

[3] K. Leo, E.O. Göbel, T.C. Damen, J. Shah, S. Schmitt-Rink, W. Schäfer, J.F. Müller, K. Köhler, and P. Ganser, Phys. Rev. B **44,** 5726 (1991); Th. Östreich, K. Schönhammer, L.J. Sham, Phys. Rev. Lett, **74,** 4698 (1995); E. J. Mayer, G.O. Smith, V. Heuckeroth, and J. Kuhl, K. Bott, A. Schulze, T. Meier, D. Benndardt, S. W. Koch, P. Thomas, R. Hey, and K. Ploog, Phys. Rev. B **50,** 14730 (1994); Y. Z. Hu, R.Binder, S. W. Koch, S.T. Cundiff, H. Wang, and D.G. Steel, Phys. Rev. B **49**, 14382 (1994).

[4] A.J. Fischer, D.S. Kim, J. Hays, W. Shan, J.J. Song, D.B. Eason, J. Ren, J.F. Schetzina, H. Luo, J.K. Furdyna, Z.Q. Zhu, T. Yao, and W. Schäfer, Phys. Rev. Lett. **73**, 2368 (1994).

[5] V. G. Lyssenko, J. Erland, I. Balslev, K. -H. Pantke, B. S. Razbirin, and J. M. Hvam, Phys. Rev. B **48,** 5720 (1993).

[6] S. Schmitt-Rink, D. Bennhardt, V. Heuckeroth, P. Thomas, P. Haring, G. Maidorn, H. Bakker, K. Leo, D.S. Kim, J. Shah, and K. Köhler, Phys. Rev B **46,** 10460 (1992).

[7] T. Yajima and Y. Taira, J. Phys. Soc. Jpn. **47,** 160 (1980).

[8] J. Lee, E. Koteles, and M. O. Vassell, Phys. Rev. B **33,** 5512 (1986).

[9] D.S. Kim, J. Shah, J.E. Cunningham, T.C. Damen, W. Schäfer, M. Hartmann, and S. Schmitt-Rink, Phys. Rev. Lett. **68,** 1006 (1992).

[10] S. Rudin, T.L Reinecke, and B. Segall, Phys. Rev. B **42,** 11218 (1992).

Figure Captions

Fig. 1. (a) Time integrated four-wave-mixing (TI-FWM) signal in the reflection geometry near the B-exciton resonance at 10, 70 and 190 K for a 7.2 micron epilayer of GaN grown on Sapphire. (b) Decay rates of FWM plotted as a function of temperature. The fit corresponds to $\gamma = 16$ μeV/K and $\Gamma_{LO} = 390$ meV.

Fig. 2. Spectrally-resolved (SR) FWM signals from the A and B exciton resonances near zero delay at 10, 50, 100, 150, and 190 K plotted together with CW reflectivity data from the same sample. The A (FX_A) and B (FX_B) intrinsic free excitons are labeled and the inset shows the excitonic band structure. The B exciton linewidth of 2.5 meV (FWHM) at 10 K together with the FWM decay time of 280 fs ($T_2 = 2\tau_{FWM}$ $\Longrightarrow$ $\Gamma_{hom} = 2.4$ meV) indicate that our excitons are mostly homogeneously broadened even at low temperature.

Fig. 3. TI-FWM data at 10 K at different detunings $\delta\omega = \hbar\,(\omega_d - \omega_2)$ meV around the B exciton. (ω_d = detection frequency). The laser is set to excite both the A and B resonances. The fact that we see no phase shift as a function of energy position across the B exciton resonance indicates that the observed beats are true quantum beats. Different temperatures are offset for clarity.

Fig. 4. TI-FWM signal at 10 K for co-linear (solid) and cross-linear (dashed) polarization geometries.

Figure 1

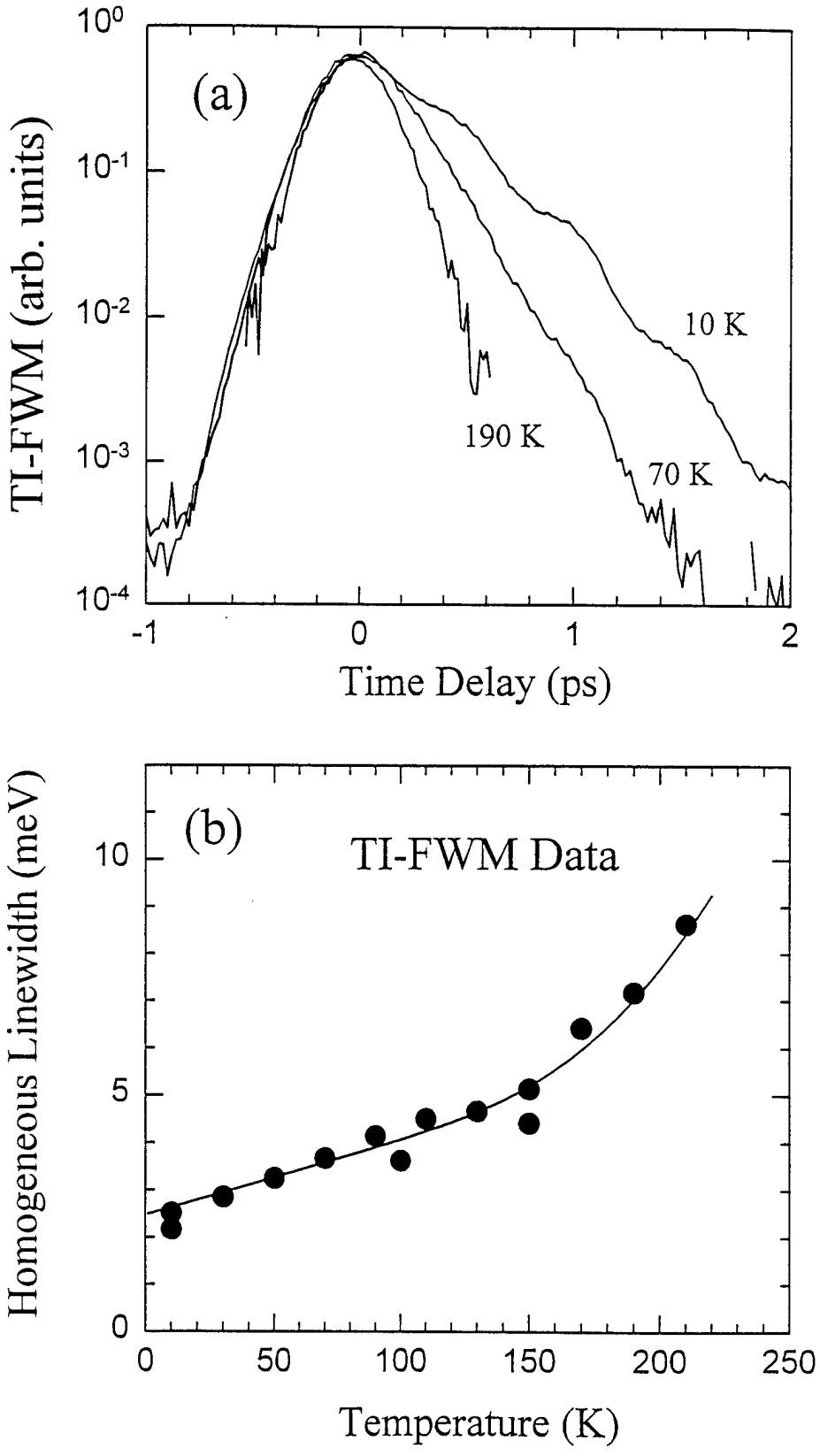
(a)
TI-FWM (arb. units)
10^0
10^-1
10^-2
10^-3
10^-4
10 K
190 K
70 K
-1
0
1
2
Time Delay (ps)
(b)
TI-FWM Data
Homogeneous Linewidth (meV)
10
5
0
0
50
100
150
200
250
Temperature (K)

Figure 2

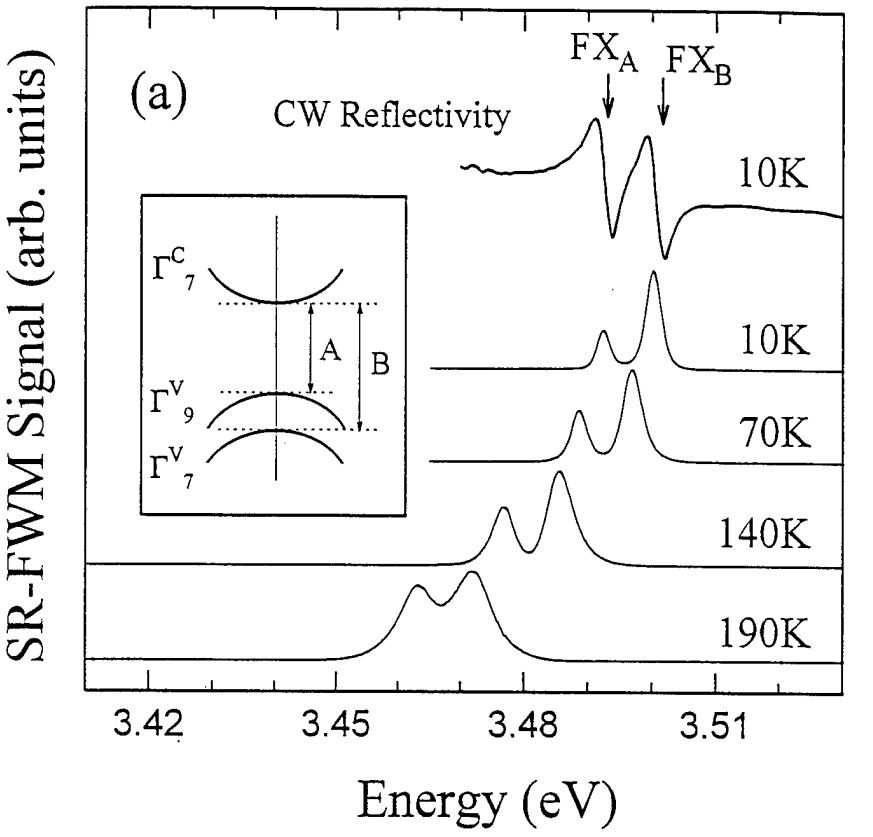
(a)
CW Reflectivity
FX_A
FX_B
10K
10K
70K
140K
190K
Γ^C_7
A
B
Γ^V_9
Γ^V_7
SR-FWM Signal (arb. units)
3.42
3.45
3.48
3.51
Energy (eV)

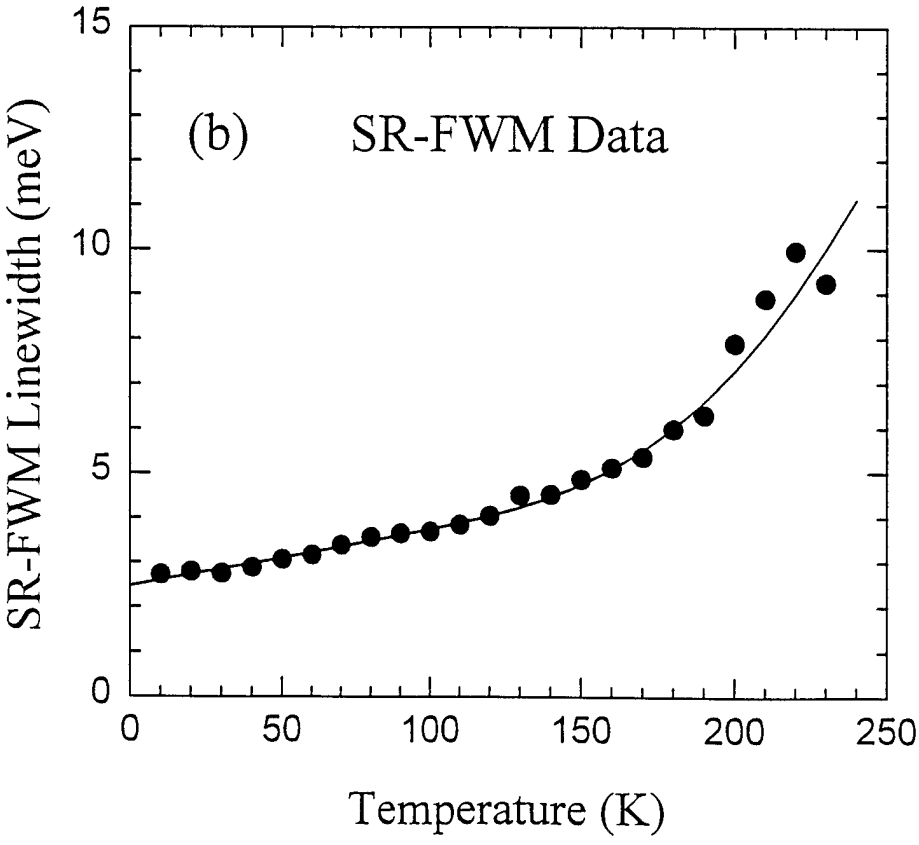
(b)
SR-FWM Data
SR-FWM Linewidth (meV)
15
10
5
0
0
50
100
150
200
250
Temperature (K)

Figure 3

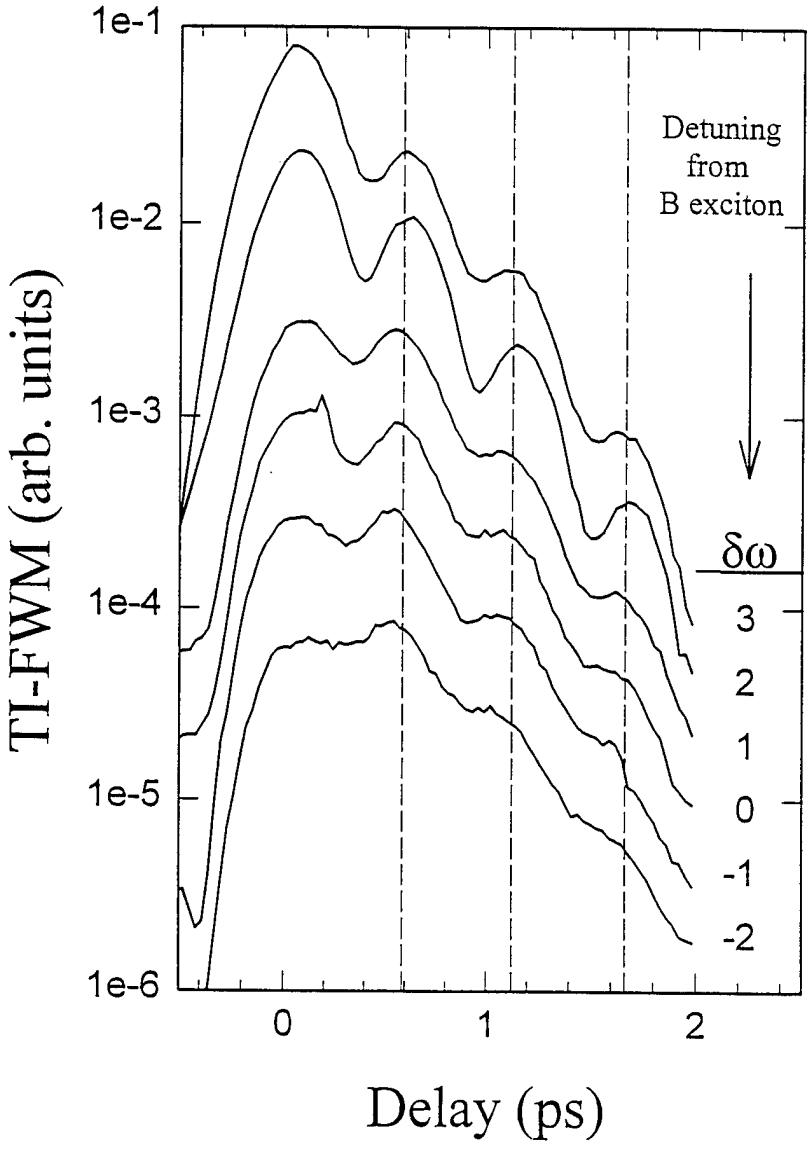
1e-1
1e-2
1e-3
1e-4
1e-5
1e-6
TI-FWM (arb. units)
0
1
2
Delay (ps)
Detuning
from
B exciton
δω
3
2
1
0
-1
-2

Figure 4

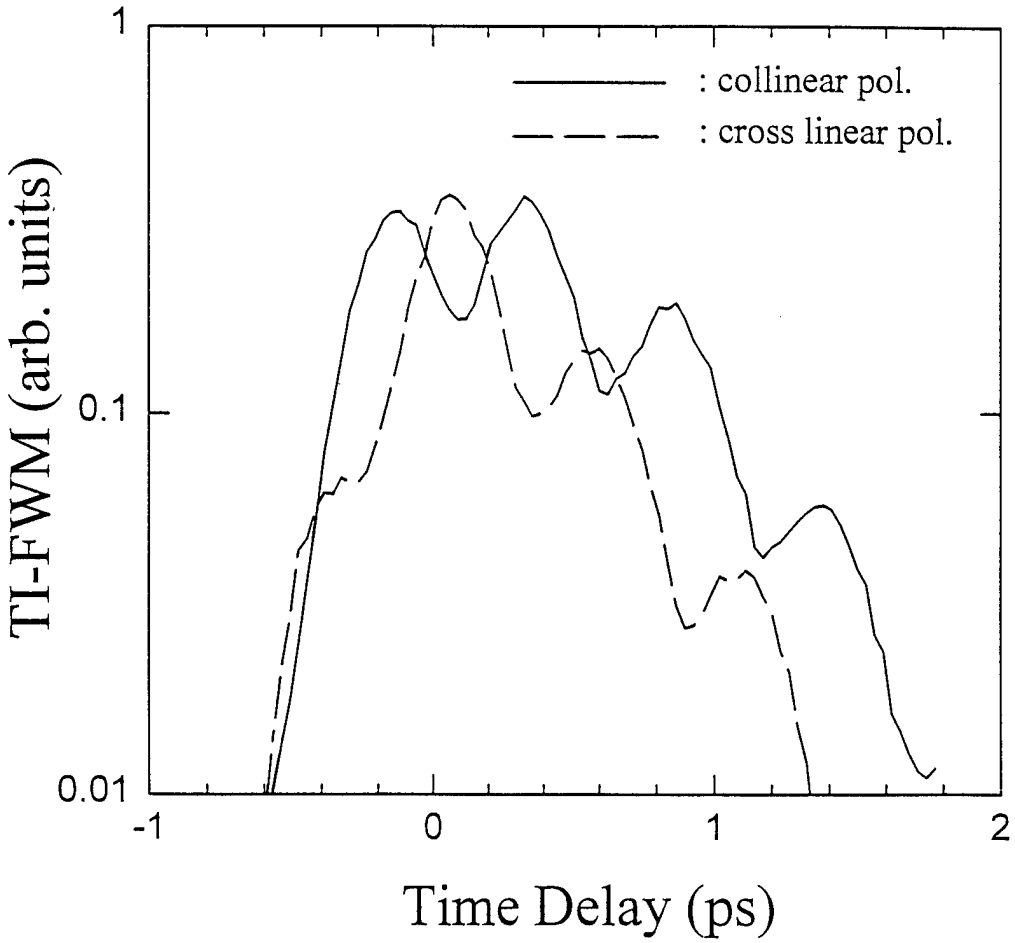
1
0.1
0.01
-1
0
1
2
TI-FWM (arb. units)
Time Delay (ps)
: collinear pol.
: cross linear pol.

Carrier Recombination Dynamics

Motivation

- To study PL decay for the intrinsic free exciton and bound exciton as well as the emissions involving defects and/or impurities
- To examine the influence of defects and impurites on the decay of exciton/carrier population
- To understand the recombination dynamics of excitons/carriers in GaN and related materials

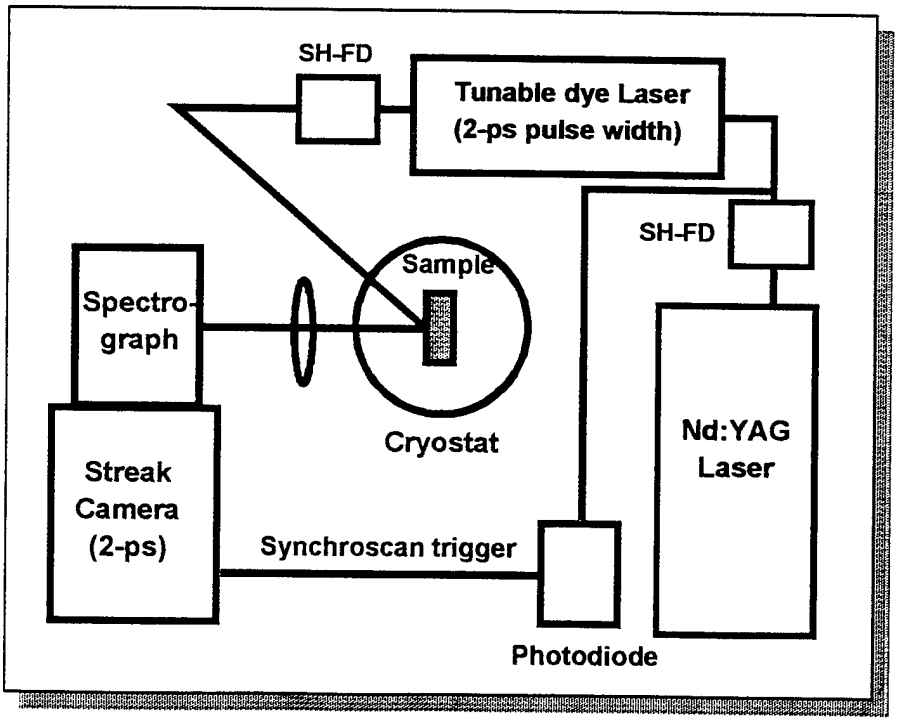

AlGaN/GaN DH structures
PL Decay time, τ

- **Exciton Wavelength Dependent**

• Above AlGaN bandgap: *Indirect GaN excitation*	*τ -- Long*
• Below AlGaN bandgap: *Direct GaN excitation*	*τ -- Short*

ISPSA 96

Carrier Relaxation/Recombination Dynamics: *AlGaN/GaN Double-Heterostructures*

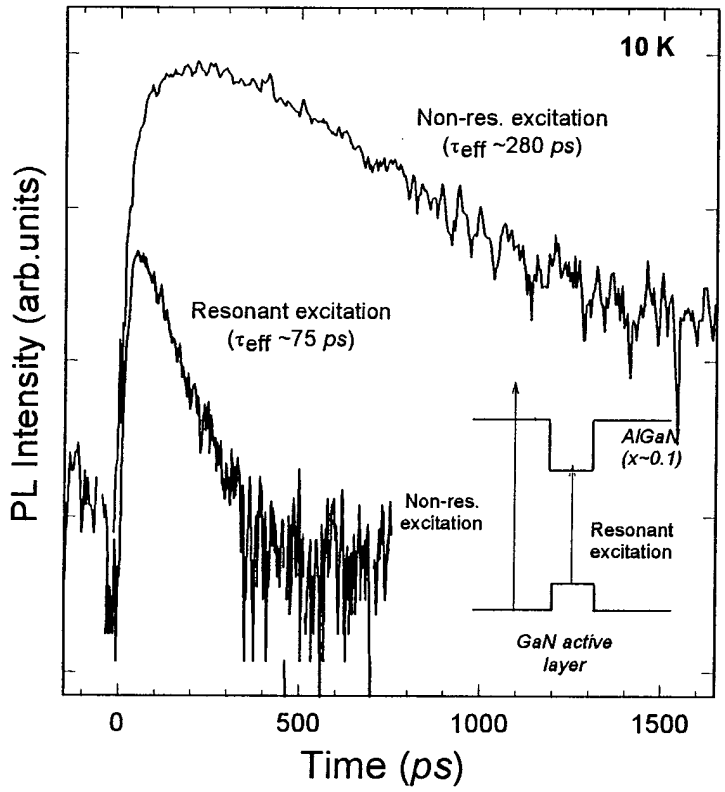

- Studied picosecond carrier relaxation and recombination dynamics in AlGaN/GaN DH structures using streak-camera method.
- A significant difference of PL decay time for exciton emission in the GaN active layer between the excitation energy above and below AlGaN bandgap:

  ~280 psec. **vs** ***~75 psec.***

- The observed increase in decay time for *above-AlGaN-bandgap* excitation is due to accumulation of photoexcited carriers in the GaN layer via carrier drifting and capture processes

ISPSA 96

Carrier Relaxation/Recombination Dynamics: *AlGaN/GaN Double-Heterostructures*

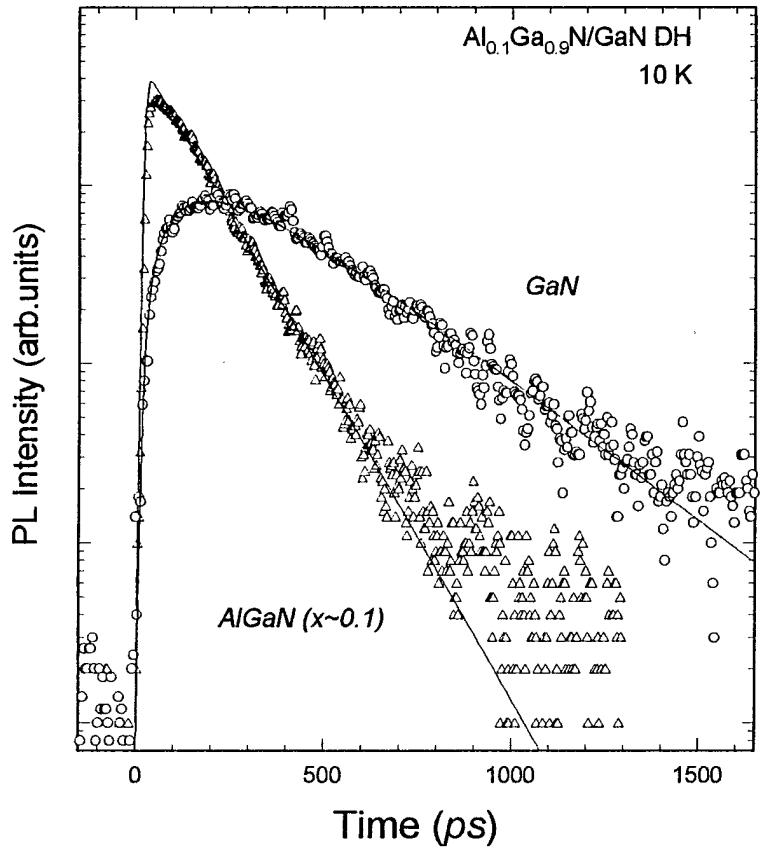

- **The dynamics of photoexcited carriers under the conditions of above-AlGaN-bandgap excitation:**

$$dn_{AlGaN}/dt = G(t) - n_{AlGaN}/\tau_{Cap} - n_{AlGaN}/\tau_{R,AlGaN}$$

$$dn_{GaN}/dt = n_{AlGaN}/\tau_{Cap} - n_{GaN}/\tau_{R,GaN}$$

- **The best fit to the experimental results using numerical fittings yields an average value of capture time:**

$$\tau_{Cap} \sim 350\ ps$$

- **The τ_{Cap} value represents an averaged carrier drifting velocity in the AlGaN cladding layer**

$$v_d \simeq d / \tau_{Cap} : \sim 6 \times 10^4\ cm/sec.$$

FEMTOSECOND FOUR-WAVE-MIXING

IN GaN

ISPSA 96

Femtosecond Four-Wave-Mixing in GaN

Coherent dynamics of intrinsic excitons in GaN probed.

TI-FWM & SR-FWM as a function of temperature

Exciton-acoustic & exciton-LO phonon interaction rates deduced.

Quantum Beats between A&B excitons observed

<First femtosecond FWM studies applied to GaN excitons>

GaN Exciton Linewidth Broadening

τ = Coherent signal decay time

$\tau = T_2/2$ for homogenous broadening

$\tau = T_2/4$ for inhomogenous broadening

Exciton linewidth accurately measured with no background via SR-FWM.

FWHM = 2.1 meV (A exciton)

2.5 meV (B exciton)

Measured τ = (0.3) psec gives:

Γ_{hom} = 2.4 meV (homogeneously broadened case)

Γ_{hom} = 1.2 meV (inhomogeneously broadened case)

Conclusion:

Excitons can be considered mostly homogeneously broadened.

Femtosecond Four-Wave-Mixing in GaN

Exciton-phonon interaction rates

$\Gamma_{hom} = \Gamma_o + \gamma T + \Gamma_{LO}/(\exp\{E_{LO}/k_bT\}-1)$

Γ_{hom} = Exciton Linewidth FWHM

LO Phonon energy = 91.7 meV

$\gamma = E_x$ - Acoustic phonon interaction rates

$\Gamma_{LO} = E_x$ - LO phonon interaction rates

Best-fit Results

Γ_o = 2.4 meV

γ = 16 μeV/K

Γ_{LO} = 390 meV

Four-wave-mixing Signals near *B*-Exciton Resonance in GaN

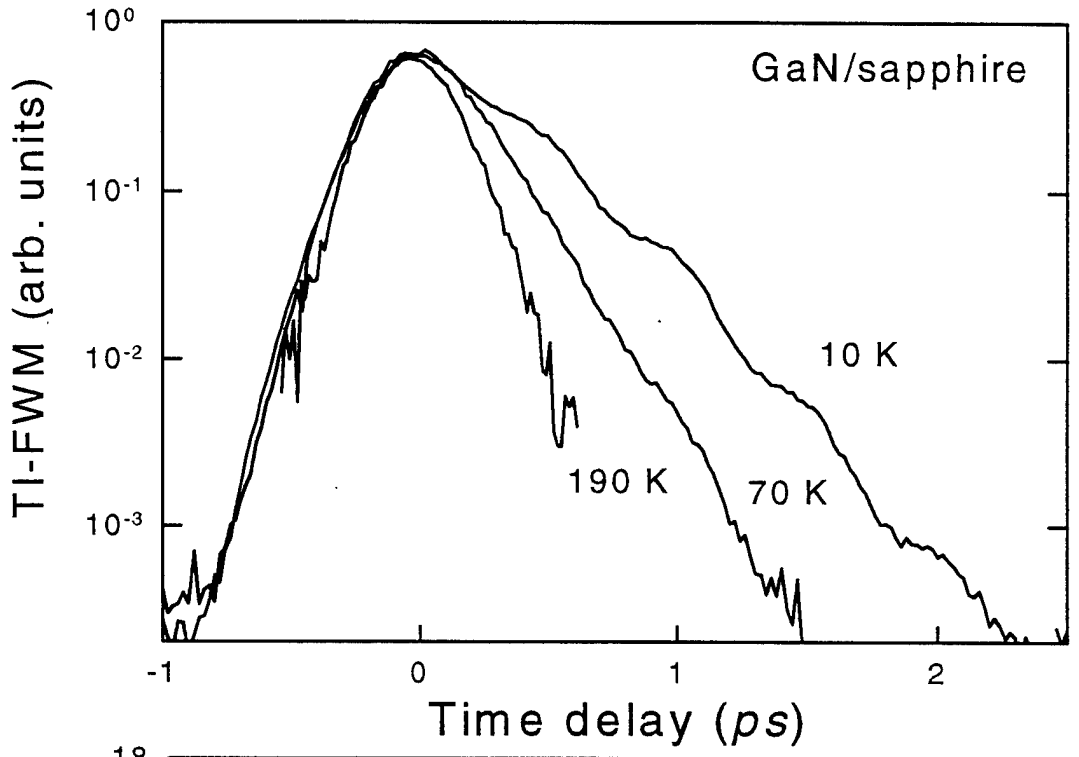

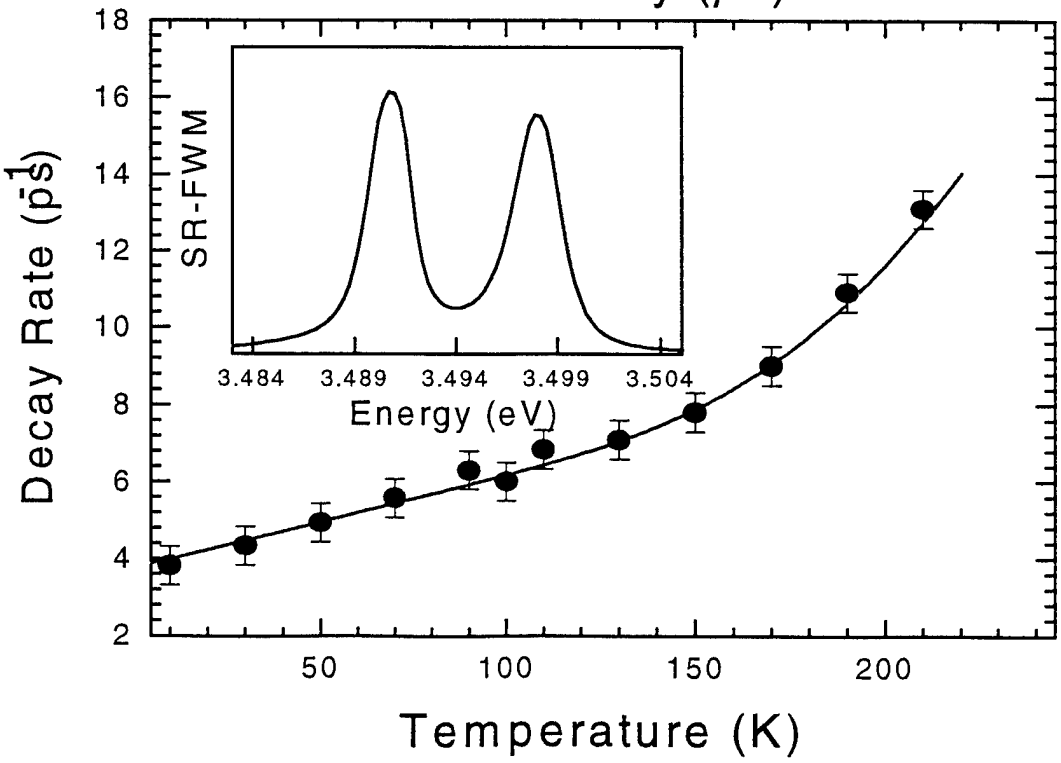

GaN Exciton Linewidth Broadening

τ = Coherent signal decay time

$\tau = T_2/2$ for homogenous broadening

$\tau = T_2/4$ for inhomogenous broadening

Exciton linewidth accurately measured with no background via SR-FWM.

FWHM = 2.1 meV (A exciton)

2.5 meV (B exciton)

Measured τ = (0.3) psec gives:

Γ_{hom} = 2.4 meV (homogeneously broadened case)

Γ_{hom} = 1.2 meV (inhomogeneously broadened case)

Conclusion:

Excitons can be considered mostly homogeneously broadened.

Quantum Beats Between A & B Exciton Levels